

The University of Sydney
Faculty of Engineering
School of Electrical and Information Engineering

Year S2, 2017

A thesis submitted in partial fulfilment of a **Master of Professional Engineering** Degree

Student Name	JIAYAO HE
SID	450428962
Unit of Study Code and Name	ELEC5021 Capstone Project B
Supervisor	XIAOKE YI
Title	Optimizing UAV via Photonic Technology

© Copyright 2013

The University of Sydney

SCHOOL OF ELECTRICAL AND INFORMATION
ENGINEERING

PROJECT CLEARANCE FORM

Unit of Study Code and Name ELEC5021 Capstone Project B

This is to certify that my student

Student Name JIAYAO HE

SID 450428962

Has:

- Returned all books and reference material;**
- Returned all equipment and keys; and**
- Tidied their work place.**

SUEIE Academic supervisor:

Signature:



Date: 03/11/2017

Name: XIAOKE YI

External supervisor (if applicable):

Signature:

Date: 03/11/2017

Name:



THE UNIVERSITY OF
SYDNEY

School of Electrical and Information Engineering

STUDENT PLAGIARISM: COURSEWORK – POLICY AND PROCEDURE

COMPLIANCE STATEMENT

INDIVIDUAL / COLLABORATIVE WORK

I certify that:

- (1) I have read and understood the *University of Sydney Student Plagiarism: Coursework Policy and Procedure*;
- (2) I understand that failure to comply with the *Student Plagiarism: Coursework Policy and Procedure* can lead to the University commencing proceedings against me for potential student misconduct under Chapter 8 of the University of Sydney By-Law 1999 (as amended);
- (3) This Work is substantially my/our own, and to the extent that any part of this Work is not my/our own I/we have indicated that it is not my/our own by Acknowledging the Source of that part or those parts of the Work.

Name(s): JIAYAO HE

SID(s): 450428962

Signature(s): 

Date: 03/11/2017

Unit of Study for which Work will be submitted:

ELEC 5021

Nature of Work submitted / unit component:

(eg, Assignment No. X; Report No. Y)

THESIS REPORT

Statement of Achievements

1. Completed design of laser power supply for UAV system
2. Completed design of video downlink communication for UVA system
3. Completed circuit and program designs of digital signal processing system
4. Completed design of PCB
5. Threes demonstrable downlink communication systems

Abstract

In past decades, the optical communication and related photonic technology has caused great concern because optical communication technology has numerous advantages such as high bandwidth, high speed of data rate and the stability of transmitting process. In order to address the power limitation of Unmanned Aerial Vehicle (UAV) and improve the stability of communication between UAV and ground station, this project and the related technologies are considered to be appropriate to meet the challenge.

This report shows multi-paths to improve the performance of the Unmanned Aerial Vehicle (UAV) in aspects of power supply and communication.

The power supply will be replaced by a high-power laser source, which has the ability to transmit power with minimized loss through optical fibre in a long distance.

The wireless communication will be replaced by optical downlink system for achieving the goal of transmitting signals with minimized attenuation and loss as well as preventing electromagnetic interference (EMI) from the environment.

Acknowledgments

I would like to acknowledge with much appreciation to people who provided me the possibility to work on this project. My dear supervisor Xiaoke Yi, who contributed to stimulating advices as well as good encouragement, gave me the project topic and guided me a lot.

Moreover, I would like to express the sincere appreciation to Shijie Song, who gave me the permission to use the related equipment and the necessary materials to complete the temperature downlink communication system.

A sincere thanks to my friend, Jianwei Zhai, who provided selfless help to me for making PCB.

Also, a special thanks to my teammate, Yichen Zhang, who cooperated with me to deal with the power design of UAV.

Last but not least, I got many thanks to the guidance given by other supervisors, who sharp my project presentation skills and gave me their comment and advices.

TOC

Statement of Achievements	iv
Abstract.....	v
Acknowledgments	vi
[List of Figures].....	ix
[List of Tables]	xii
[Glossary]	xiii
1. Introduction	1
2. Background	2
3. Design	5
3.1 Laser Power Supply	5
3.1.1 System Overview.....	5
3.1.2 High-Power UAV Selection	5
3.1.3 Laser Power Kit.....	7
3.1.4 DC Converter for High-Power Drones.....	8
3.1.5 Conclusion	11
3.2 Video Optical Downlink Communication System	12
3.2.1 System Overview.....	12
3.2.2 USB 3.0 optical cable for video camera.....	12
3.2.3 FPV camera.....	14
3.2.4 FPV to USB Linker.....	16
3.2.5 Conclusion	16
3.3 Temperature Optical Downlink Communication System	17
3.3.1 System overview.....	17
3.3.2 Temperature sensor.....	18
3.3.3 Signal Processor	20
3.3.4 USB to TTL converter.....	21
3.3.5 Circuit & Program design of signal processing	24
3.3.6 Further design.....	33
3.3.7 Light source	37

3.3.8	Photovoltaic converters	40
3.3.9	Final version control.....	42
3.3.10	Conclusion.....	43
4.	Analysis & Test.....	44
4.1	Original Outputs from The Temperature Sensor.....	44
4.2	Converted output from the IF D96F	46
5.	Conclusion.....	48
5.1	Completed works	48
5.2	Future work	49
6.	Appendix.....	A-1
7.	Bibliography.....	A-A

[List of Figures]

Figure 1. The impact of applying an AWGN channel to an OFDM radio system	3
Figure 2. Optical fibres is Immune to EMI	3
Figure 3. Initial UAV System Scheme	5
Figure 4. Simtoo Dragonfly Drone Pro	6
Figure 5. AOI-PT6-FC-0-B laser source [9]	7
Figure 6. The I-V curve of laser power kit [9]	8
Figure 7. APXW012A0X3-SRZ DC-DC converter [11].....	9
Figure 8. The operation scheme of laser power system.....	11
Figure 9. Architecture of the proposed video optical downlink.....	12
Figure 10. AOC-ACS2CVA050M20	13
Figure 11. The interior structure of AOC-ACS2CVA050M20.....	13
Figure 12. Operation of AOC-ACS2CVA050M20	14
Figure 13. Storm 2g CC1563 Micro FPV Camera (140°)	15
Figure 14. FuriousFPV-Acc-FPV-0157-S [17].....	16
Figure 15. The operation scheme of Video Optical Downlink Communication System	16
Figure 16. Architecture of the proposed temperature optical downlink	18
Figure 17. DS18B20 block diagram [20]	19
Figure 18. Block diagram of STC89C52.....	20
Figure 19. Standard A plug USB	22
Figure 20. CH340G	23
Figure 21. Circuit of the processor [23]	25
Figure 22. Circuit of the sensor	25
Figure 23. Simulation of the circuit.....	26
Figure 24. The System Flowchart.....	27
Figure 25. The constructed circuit on breadboard	31
Figure 26. The original hexadecimal data received.....	31
Figure 27. The decoded data received.....	32

Figure 28. Initial connection scheme of the signal processing system	33
Figure 29. Soldering board temperature signal processing system.....	33
Figure 30. Circuit of the processor with LCD displayer [34]	34
Figure 31. PCB design on Altium Designer.....	35
Figure 32. PCB of the temperature signal processing system.....	37
Figure 33. IF E93	38
Figure 34. Forward current vs. forward voltage [38].....	39
Figure 35. Typical spectral output vs. wavelength [38].....	39
Figure 36. Test/Application circuit (IF = 33mA) [38].....	39
Figure 37. Cross-section of fiber optic device [38].....	39
Figure 38. IF D96F	40
Figure 39. Normalized threshold irradiance vs. amb. temp [40]	42
Figure 40. Typical operating circuit [40]	42
Figure 41. Integrated temperature communication optical downlink system.....	42
Figure 42. The system scheme of temperature downlink communication system	43
Figure 43. The output of the sensor (18.2°C)	44
Figure 44. The output of the sensor (18.5°C)	44
Figure 45. The output of the sensor (18.7°C)	44
Figure 46. The output of the sensor (19.0°C)	44
Figure 47. The output of the sensor (19.3°C)	44
Figure 48. The output of the sensor (19.5°C)	44
Figure 49. The output of the sensor (19.8°C)	45
Figure 50. The output of the sensor (20.3°C)	45
Figure 51. The output of the sensor (20.5°C)	45
Figure 52. The output of the sensor (20.7°C)	45
Figure 53. The output of the sensor (21.5°C)	45
Figure 54. The output of the sensor (22.0°C)	45
Figure 55. The output of the sensor (22.3°C)	45
Figure 56. The output of the sensor (22.5°C)	45
Figure 57. Environment Temperature V.S. the Sensor Output Voltage.....	46

Figure 58. The output of the IF D96F (18.5°C).....	46
Figure 59. The output of the IF D96F (20.5°C).....	46
Figure 60. The output of the IF D96F (22.5°C).....	47
Figure 61. The output of the IF D96F (24.5°C).....	47
Figure 62. The output of the IF D96F (26.5°C).....	47
Figure 63. The output of the IF D96F (28.5°C).....	47
Figure 64. Environment Temperature V.S. the amplified Output Voltage	47
Figure 65. PCBlayout of DIMOTO board	A-1

[List of Tables]

Table 1. The Specifications of Simtoo Dragonfly Drone Pro Drone [5].....	6
Table 2. DC converter for high-power requirement [11].....	11
Table 3. Specifications of AOC-ACS2CVA050M20 [13]	13
Table 4. Specifications of 2g CC1563 Micro FPV Camera (140°) [16]	15
Table 5. DS18B20 Temperature Sensor [20].....	19
Table 6. Specifications of 89C52 [23].....	21
Table 7. Basic specifications of CH340G [25].....	24
Table 8. Characteristics of IF E93 (TA =25°C).....	39
Table 9. Features of IF-E93 led [38].....	39
Table 10. Characteristics of IF D96F (TA=25°C) VCC = 4.75 to 5.25 V [40]	41

[Glossary]

Words	Meaning
Unmanned aerial vehicle (UAV)	In this project, the UAV refers to the drone, an air craft controlled by ground-based controller and has a communication system transmitting signals between the PC ground station and the drone.
Downlink system	In this project, the downlink system means the link sending data from the drone down to the ground station.
Single Chip Microcomputer (SCM)	Also known as microcontroller chips used in embedded devices. It provides basic functionality of processing signals from the downlink system.
C language	The main language utilized by SCM.
Optical-to-electrical (O/E) and electrical-to-optical (E/O)	The photonic technology that transfers optical signals to electrical signals and vice versa.
Electro-Magnetic Interference (EMI)	It is also called radio-frequency interference (RFI), a disturbance generated by external sources, such as radio, signal jammer and power transmission, which may affect the wireless communication system of UAV.

1. Introduction

The main propose of this project is researching the possibility of implementing photo-electronic technique, such as power over fibre (POF) and optical communication on the tethered UAV system for improving the system performance. Speak in more details, this project can be separated into two parts [1].

The first one is utilizing optical fibre and high-power laser source to power the whole UAV system. Power over fibre (POF) is a kind of photonic technology in which a laser source sends laser though a fibre optic cable as an energy source. However, we found the needed power of the laser source is too high to be implemented under the laboratorial condition, which is from 22.2W to 75W. At the such power level, laser can be extremely dangerous to operate in laboratory environment. Thus, we only analyse the theoretical possibility of how to power the drone with laser source as well as research the suited system components on global market.

The second one is optical downlink communication system. The propose of the optical downlink is receiving sensing signals from the UAV system. In this project, the temperature downlink communication system has been successfully built and tested. The theoretical design of the video downlink system has been completed and analysed.

The potential issues, such as communication jamming, wireless security, limitation of data rates, stability and intensity of signals are main open issues which will reduce the system performance and lead to security uncertainty. This report will discuss possible solutions which may overcome these issues and enhance the system performance in aspects of communication efficiency and security.

This report is written in chronological sequence.

2. Background

Wireless is the nowadays mainstream technology applied on Unmanned Aerial Vehicle (UAV), while tethered drones are specifical to be utilized in some special situations, such as military realm, camp monitoring and intense electromagnetic interference environment. In such situations, wireless UAV may lose control, be hacked by enemy or be forced landing because of the power limit, immunity to EMI, and the inadequate energy source (the working period of a normal 3S battery of wireless UAV is normally from 5 mins to 20 mins) [2]. Thus, the advantages of tethered UAV are irreplaceable in aspects of stabilization and continuous working period.

However, the normal tethered UAV are generally powered via electrical cables which are too heavy to restrict the maneuverability of the UAV since the carrying load of the flying drone is limited. Thus, utilizing optical fibre as the medium between the drone and the ground station is a considerable and feasible way to improve the maneuverability of the UAV since the normal weight of optical fibres is generally less than electrical cables [3]. The core diameter of a common type multi-mode fibre is normally greater than 10 micro-meters and the core diameter of a general single-mode fibre is around 8-10 micro-meters. Compared to coaxial cables, optical fibres have greater bandwidth, and require less insulation and jacketing [3].

Meanwhile, wireless communication between the drone and the ground station may be affected by EMI [4]. There are many of wireless systems operating in the adjacent frequency or in the same bands. These operations may result in an electromagnetic interference (EMI), which can degrade the performance of wireless systems. There are three types of EMI sources, which are natural, intentional, or non-intentional. A result of an existence of a radar system can emit high-level power, which can be considered as the intentional interference. The interference coming from non-communication systems, such as monitors, power and medical equipment lines, is

the non-intentional interference. The performance of a radio system can be effected badly by EMI, which can lead to an equipment to be malfunction [4].

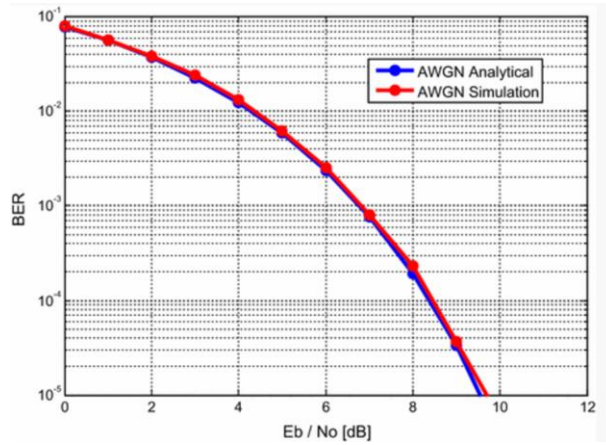


Figure 1. The impact of applying an AWGN channel to an OFDM radio system

The figure above shows the impact of applying an additive white Gaussian noise (AWGN) channel to an Orthogonal Frequency Division Multiplexing (OFDM) radio system. As the figure shows, the performance of the radio system is significantly degrading while the level of the noise is increasing.



Figure 2. Optical fibres is Immune to EMI

Optical fibres can use pulses of light to transmit signals in the threads of glass. They are non-metallic and immune to radio frequency interference as well as electro-magnetic interference. Also, the attenuation loss of fibres is as low as 0.2db/km. Thus, replacing the wireless communication system to the optical communication system with related photonic technology is significative and feasible to implement.

Furthermore, there are many factors that can limit the range and the data rates of wireless video downlink system. As the increase of the distance between the drone and the ground station, the path loss will diminish the signal intensity. Also, obstacles between the transmitting lines can make additional attenuation. Thus, further researches about the potential solutions of how to deal with these issues above and improve the performance of the downlink system are valuable to be present.

3. Design

3.1 Laser Power Supply

3.1.1 System Overview

The whole system scheme is shown in the figure 1 below.

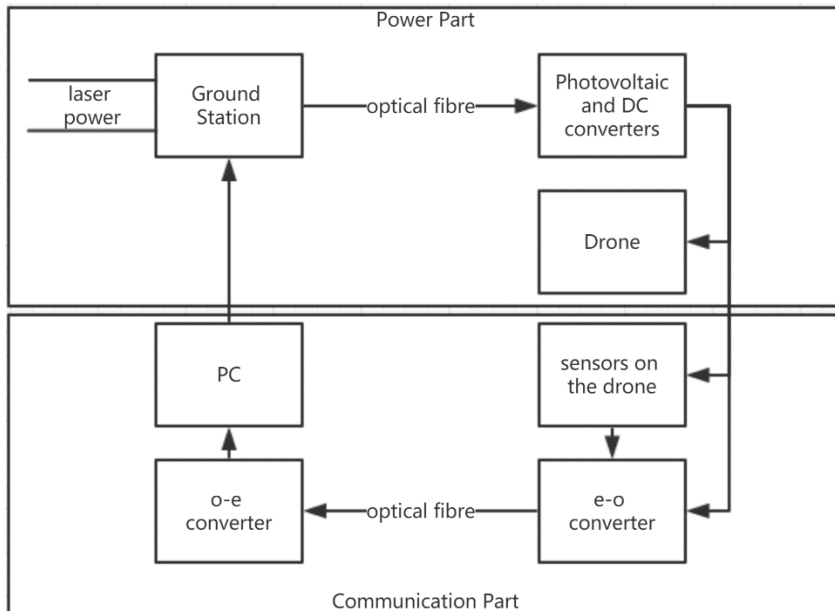


Figure 3. Initial UAV System Scheme

The operation of the whole optical tethered UAV system is shown in the figure above. In the initial design, the laser power will be converted into electrical power by the optical-electrical photovoltaic converters to supply the power system of the UAV as well as the optical communication part. The power of the camera could be supplied by the converted electrical power whilst the sensor information could be transferred to photonic signals via an electrical-optical converter and pass through optical fibre then received by an optical-electrical converter. Finally, the sensor information would be displayed on PC screen.

3.1.2 High-Power UAV Selection

There are various kinds of drones on the market, which have different sizes, power requirements, maximum carry loads, and functions. However, the drones used in this project should have brushless motors since the brushed motors may burn out

under the long-period working condition. After compared with different types of drones, the potential drone with brushless motors we selected in the first testing step is QX130, which indicated by the other teammate. A small-size, low power and minimized carry load drone which can be utilized in the first testing step. The advantage of small drone is that it can be easily powered and operated in the laboratory environment for obtaining experimental data. The drawback is apparently shown that the carry load is too small to allow it flying with additional components. For high-power and maximum carry load in the real operating condition, the selected feasible drone is shown below.



Figure 4. Simtoo Dragonfly Drone Pro

Unfold Dimension:	32*32*16 cm
Aircraft Weight (with gimbal+camera+propellers+battery):	1200g
Max Payload:	400g
Max Take-off Weight:	1500g
Wingspan:	400mm
Motor: 2212	75W Brushless Motor
Max Flight Altitude (above sea level):	4000 m
Battery Capacity	5200mAH
Voltage	11.1V

Table 1. The Specifications of Simtoo Dragonfly Drone Pro [5]

As the table shown above, the Simtoo Dragonfly Drone Pro drone has the higher performance in term of carrying load. The advantage is that it can completely satisfy the requirement for real operating condition. However, the drawback is that it needs more power to supply the 75W brushless motors. If it uses laser power, the following issues in aspects of the safety and the capability of fibre are needed to be seriously considered.

3.1.3 *Laser Power Kit*

In the initial design, we decided to power the UAV system through converting laser power into electrical power via the photovoltaic converters. The advantages of Power over Fibre include electrical insulation and immunity to EMI [6]. Meanwhile, the weight of fibre is about a fifth of the weight of electrical cable so that the carrying load of UAV could be minimized [7]. Nevertheless, the limiting factors of laser power include the coupling efficiency, the o-e converting efficiency and the high payload due to the heat sinks of the receiver [8].

After thoroughly searched the market, the most suitable one we found is AOI-PT6-FC-0-B laser power kit which is shown in the figure below.



Figure 5. AOI-PT6-FC-0-B laser source [9]

In order to satisfy the required power need, we need to combine a number of AOI-PT6-FC-0-B kits to obtain over than 20W of output power [9].

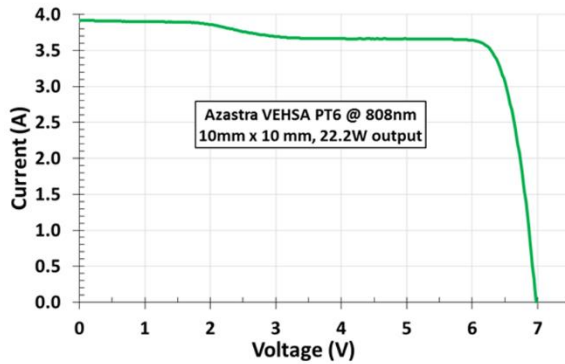


Figure 6. The I-V curve of laser power kit [9]

We can indicate the relation between the output current and the output voltage from the figure 4 above. The laser kit operating at 808nm, 22.2W has 3.5A output current and 6.2V output voltage. Also, there is a laser source whose output power can up to 75W. These laser sources are potentially suited for the real operating condition while the risk of this level of high laser power may be unexpected so it is not considered by our supervisor at the testing step in laboratory.

3.1.4 DC Converter for High-Power Drones

In order to satisfy the accurate voltage output, DC converters are essential components in UAV system. The photovoltaic converter will transfer laser power from the laser source to electrical power with various voltages, while the voltage requirement of the selected small UAV is 3.7V. Meanwhile, the flight dynamic of the UAV is limited by various elements, such as the maximum power of the laser source, transferring efficiency, the carrying ability of UAV as well as load components, so the DC converters installed on UAV must be as light as possible to minimize the weight of UAV. Thus, an adjustable, light with high-efficiency DC-DC converter is required to supply the UAV power.

Since we may need the high-power drone, DC-DC-boost converters are considered in the future steps. However, most of boost converters we could find on the market running at over than 10A required cooling equipment, such as fans or heat sinks. Namely, their weights are normally over than 150 grams, which is too much higher

than the carrying load of drones. Thus, we need to consider an alternative way to achieve high output voltage requirement.

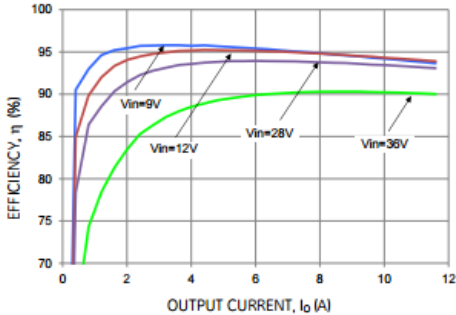
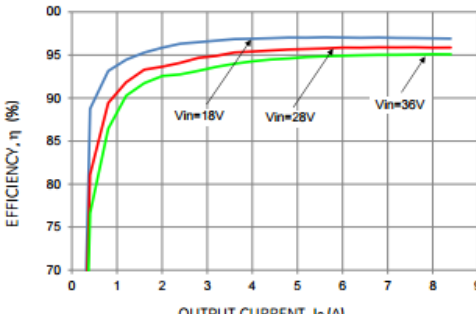
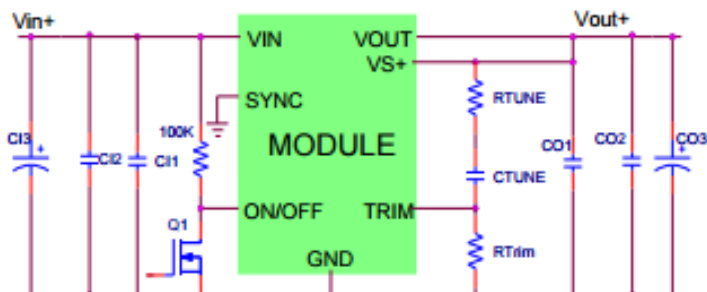
In order to gain high output voltage with high output current as well as high-efficiency, we consider paralleling several photovoltaic receivers to transfer power from multiple laser sources. Thus, the voltage transferred by photovoltaic receivers can reach higher. Meanwhile, we decide to utilize a high efficiency DC-DC step-down converter, which can handle high output current to buck the voltage to meet specific voltage requirements of drones [10]. In this way, the demand to DC-DC boost converter can be eliminated.

In order to satisfy other specific drones which running at high-voltage, a suited DC-DC buck converter with high output current is required. The specifications of the required DC-DC buck converter that we found online is shown in the table below.



Figure 7. APXW012A0X3-SRZ DC-DC converter [11]

Name	APXW012A0X3-SRZ
Input voltage(V)	9 V to 36 V
Output voltage(V)	3 V to 18 V
Maximum output Current(A)	12A
Max power (W)	Up to 56W
Size	33 mm x 13.46 mm x 10 mm
Weight(g)	7g

Operating temperature(° C)	-40 to 85°C
Applications	Distributed Power Architectures Intermediate Bus Voltage Applications Telecommunications Servers and Storage Applications Networking Equipment Industrial Equipment
Efficiency	Around 94% when the output voltage is 5V  <p>The graph plots Efficiency (η) in percent against Output Current (Io) in Amperes. Four curves are shown for different input voltages: Vin = 9V (blue), Vin = 12V (red), Vin = 28V (green), and Vin = 36V (purple). All curves show efficiency increasing with output current and plateauing around 94% at higher currents.</p> Around 96% when the output voltage is 12V  <p>The graph plots Efficiency (η) in percent against Output Current (Io) in Amperes. Three curves are shown for different input voltages: Vin = 18V (blue), Vin = 28V (green), and Vin = 36V (purple). The 36V curve shows the highest efficiency, reaching nearly 98% at 8A.</p> The higher output voltage, the higher efficiency
Operating circuit	

Datasheet	http://www.mouser.com/ds/2/167/APXW012_DS-537356.pdf
-----------	---

Table 2. DC converter for high-power requirement [11]

According to the datasheet, the experimental results only show two points which indicate the relation between output voltage and output current. Thus, the recommended values for 11V output can be estimated as:

$$R_{trim}=11.44K\Omega, C_0=1\times22\mu F+1\times330\mu F, R_{tune}=300\Omega, C_{tune}\approx1100Pf, \nabla V_o\approx2\%$$

The parameters above are only recommended values and need to be adjusted based on the experiment.

3.1.5 Conclusion

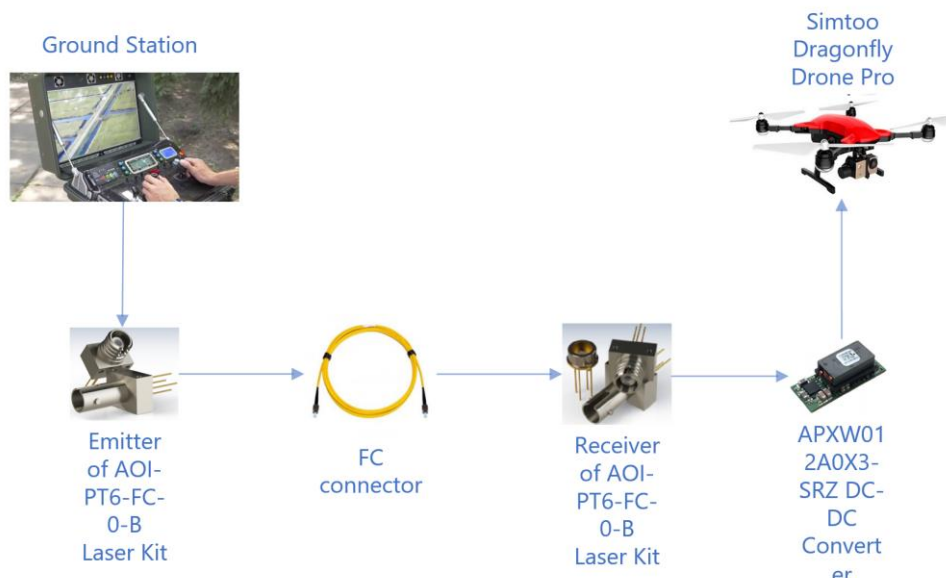


Figure 8. The operation scheme of laser power system

As the figure shown above, the operation scheme of laser power system can be described as follow. The ground station will power the emitter of AOI-PT6-FC-0-B laser source and generate high-level of laser, then the laser will pass though the FC connector and received by the receiver of AOI-PT6-FC-0-B laser kit. Once, the laser is power is converted to electrical power, the APXW012A0X3-SRZ DC-DC converter can modify the electrical voltage to fulfill the voltage need of the Simtoo Dragonfly Drone.

However, the power need of brushless motor of the Simtoo Dragonfly Drone is up to 75W. Namely, the need of laser power is up to 150W, which is needed to parallel at least 7 AOI-PT6-FC-0-B laser kits. The operation is dangerous and may damage the fibre as well as connectors.

3.2 Video Optical Downlink Communication System

3.2.1 System Overview

The function of this optical downlink is converting the video signals from the video camera on UAV to optical signals then send them to the PC ground station via optical fibre. Once the optical signals are received by the ground station, they will be converted back to video signals and present on the PC ground station [12]. The basic system scheme of the video optical downlink is shown in the figure below.

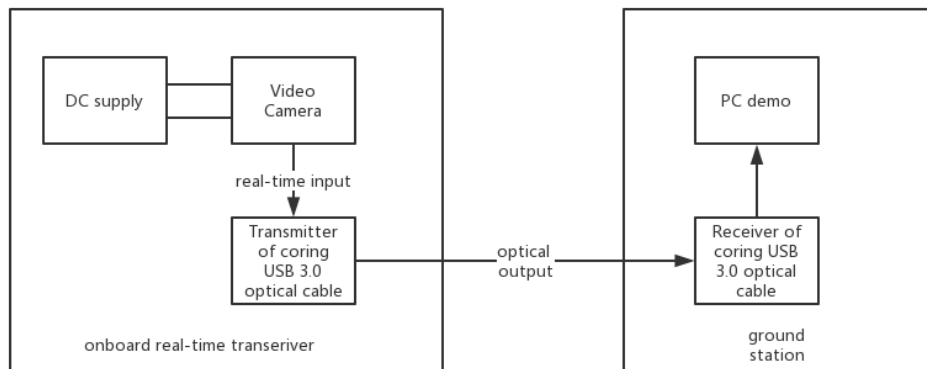


Figure 9. Architecture of the proposed video optical downlink

3.2.2 USB 3.0 optical cable for video camera

The optical cable for video camera should have the ability to converter video signals to optical signals with high speed of data rate and have the compatibility to both video camera and PC ground station. Also, it should be light and strong enough to carry on the UAV.



Figure 10. AOC-ACS2CVA050M20

The figure above shows the selected USB 3.0 optical cable, AOC-ACS2CVA050M20, which can be utilized in this project. It has the high transmitting speed (up to 5Gb/s data rate) and long operating distance (50 meters). Moreover, its integrated circuit has the ability to convert electrical signals to optical signals and vice versa.

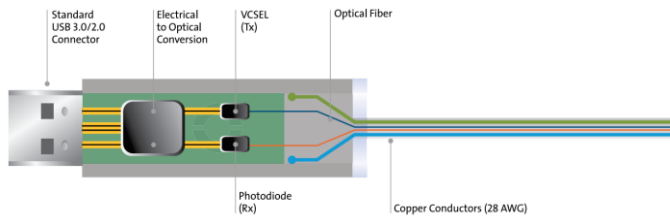


Figure 11. The interior structure of AOC-ACS2CVA050M20

As the figure 8 shows above, the AOC-ACS2CVA050M20 has a standard USB 3.0/2.0 connector, an electrical to optical (E/O) as well as optical to electrical (O/E) converter, a optical transmitter and receiver which are connected to optical fibre.

AOC-ACS2CVA050M20	
Transmitting distance	50 meters/165 ft
Connector type	Type A plug to Type A receptacle
Operating Temperature	0° to 45°C (32° to 113°F)
Price	\$499 American dollars

Table 3. Specifications of AOC-ACS2CVA050M20 [13]

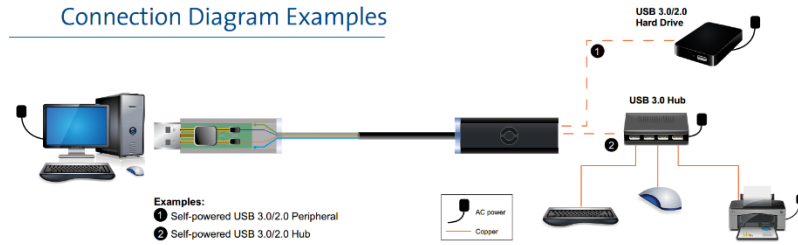


Figure 12. Operation of AOC-ACS2CVA050M20

The AOC-ACS2CVA050M20 can be utilized with multi-devices who have USB 3.0/2.0 standard connectors.

3.2.3 FPV camera

The camera utilized on the UAV should be small, lightweight and be able to send real time video back down to the PC ground station via the optical cable. First Person View (FPV) camera is smaller, lighter and has less latency compared to HD camera. Typically, the latency of HD cation camera like GoPRO is 100ms to 200ms, which is hard to notice while flying. However, a 100ms delay when flying at 50mph means the drone will travel about 1.7meters before the ground station receives the video signals [14]. The FPV system has much lower latency, which is less than 40ms. Moreover, the type of sensor utilized on FPV camera is Complementary Metal Oxide Semiconductor (CMOS) camera. The advantages of CMOS camera compared to normal charge-coupled-device (CCD) camera include higher resolution, higher frame rate, better colour performance, less power requirement and generally cheaper to make [15].

Thus, the FPV camera is a better choice for this project.

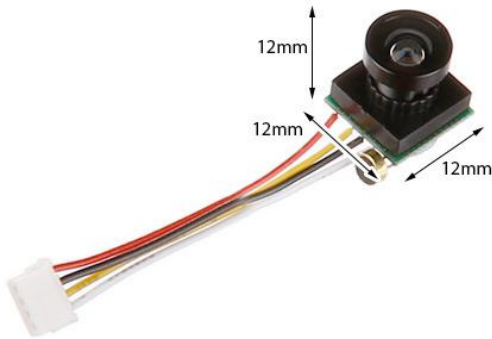


Figure 13. Storm 2g CC1563 Micro FPV Camera (140°)

The camera shown in the figure above is Storm 2g CC1563 Micro FPV Camera (140°), which is made for FPV with 600TV line high quality image. It performs well in bright and dark environment with only 12 x 12 mm micro size and 2 grams weight. Thus, it is a good choice for obtaining video data in the sky.

Storm 2g CC1563 Micro FPV Camera (140°)	
Pin assignment	
FOV	140 degrees
Resolution	600TVL
Power	DC 5V
Camera dimension	12 x 12 x12 mm
Camera weight	2 grams

Table 4. Specifications of 2g CC1563 Micro FPV Camera (140°) [16]

3.2.4 FPV to USB Linker

For linking the FPV camera and the USB 3.0/2.0 optical cable, a FPV to USB Linker is needed. The figure shows below is the selected FPV to USB Linker, which is FuriousFPV-Acc-FPV-0157-S.

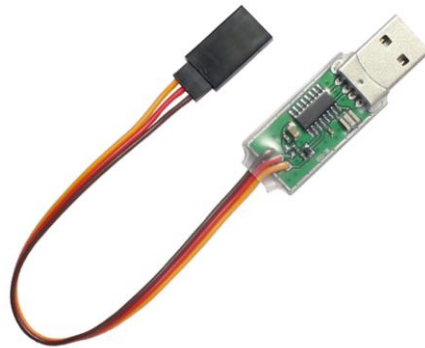


Figure 14. FuriousFPV-Acc-FPV-0157-S [17]

The FuriousFPV-Acc-FPV-0157-S FPV to USB linker above is able to help the Storm 2g CC1563 Micro FPV Camera (140°) link to the AOC-ACS2CVA050M20 USB optical cable.

3.2.5 Conclusion

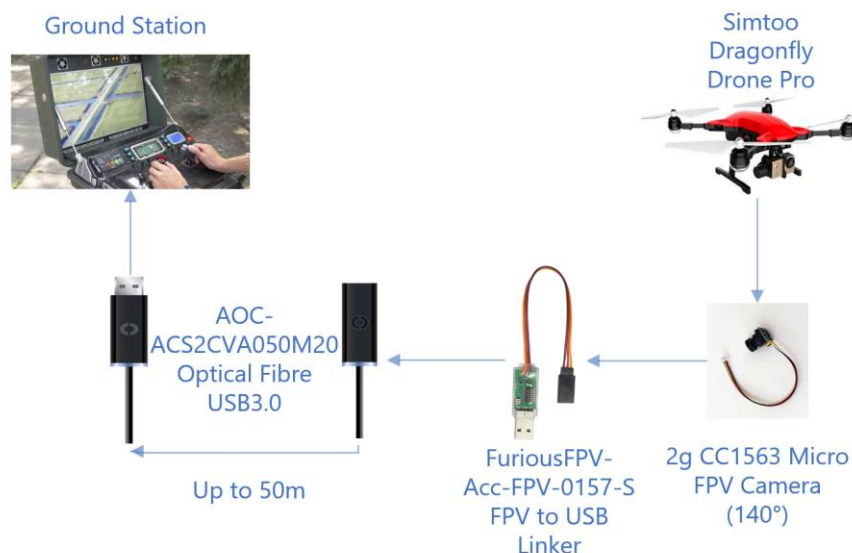


Figure 15. The operation scheme of Video Optical Downlink Communication System

As the figure shown above, the video sensor CC1563 Micro FPV Camera is connected and to the drone for power supply. Then the video signals from the FPV camera will be transferred via the FPV to USB linker to the emitter of AOC-ACS2CVA050M20 optical cable. The electrical video signals will be converted to optical signals and transmitted through the optical fibre then received as well as converted back to electrical signals by the receiver of AOC-ACS2CVA050M20. Finally, the PC ground station is able to receive and display the real-time video from the drone.

The design of the video communication downlink system had been completed in 20 August 2017. The components include: AOC-ACS2CVA050M20 USB 3.0/2.0 optical cable, Storm 2g CC1563 Micro FPV Camera (140°), and FuriousFPV-Acc-FPV-0157-S FPV to USB linker. The estimated total cost is: \$635 or \$499 in American dollars (optical cable) + \$ 20.12 (FPV camera) + \$13.43 (FPV to USB linker) = \$668.55 Australia dollars.

3.3 Temperature Optical Downlink Communication System

Since the design of video communication optical downlink system was completed, the external supervisor Shijie Song, advised to build a demo-version of the optical downlink system and provided a DS18B20 temperature sensor. The task of building a downlink system based on a sensor is much harder than the previous video downlink system, because the underlying function of digital signal processing should be resolved with an embedded system, which can process the sensor signals to be acceptable by PC ground station.

3.3.1 *System overview*

The function of this optical downlink is converting sensor signals from the sensing element on UAV to optical signals then send them to the ground station via optical fibre. Once the optical signals are received by ground station, these optical signals will be converted to electric signals and processed by the signal processor as digital

signals which can be accepted by PC. The basic system scheme of the temperature optical downlink is shown in the figure below [18].

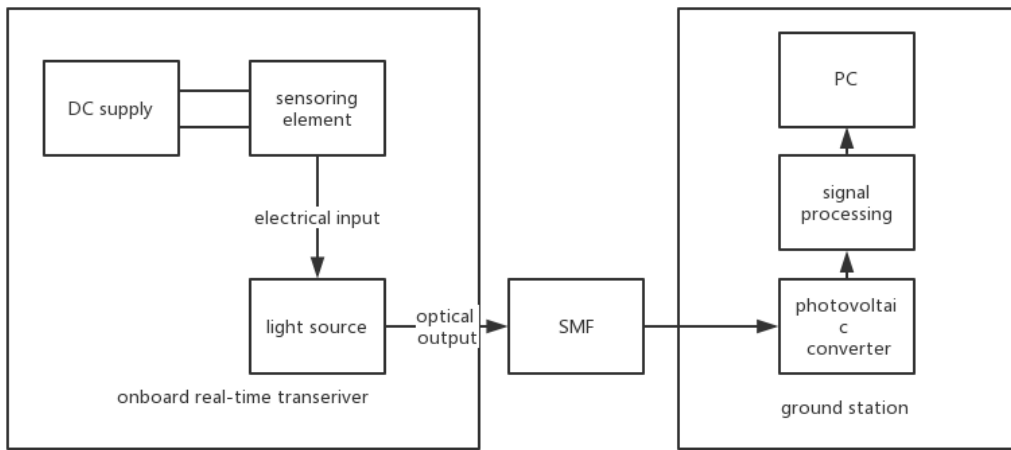


Figure 16. Architecture of the proposed temperature optical downlink

In order to achieve a secure and fast optical downlink of tethered UAV, a temperature downlink system is assigned to me by the external supervisor to design for verifying the theory of optical downlink system of tethered UAV.

3.3.2 Temperature sensor

It is a Digital thermometer who has the temperature measurements of 9bit to 12bit Celsius and the user-programmable lower and upper triggered points alarming function. The unique 1-wire interface of the sensor requires with only one port pin for communication. A unique 64-bit serial code is contained in the on-board ROM of the sensor, which allows one wire bus to communicate with multiple sensors. The sensor communicates over 1-wire bus with one data line to transfer signals to a signal processor. Moreover, the sensor can be operated with the power from data line, so there is no need to power it with external power supply [19].

DS18B20	
Pin assignment	<p>PIN ASSIGNMENT</p> <p>DS18B20 To-92 Package DS18B20Z 8-Pin SOIC (150 mil)</p>
Power supply range	3.0V to 5.5V
Measures temperature range	-55°C to +125°C
Speed	Convert 12-bit temperature to digital word in 750ms

Table 5. DS18B20 Temperature Sensor [20]

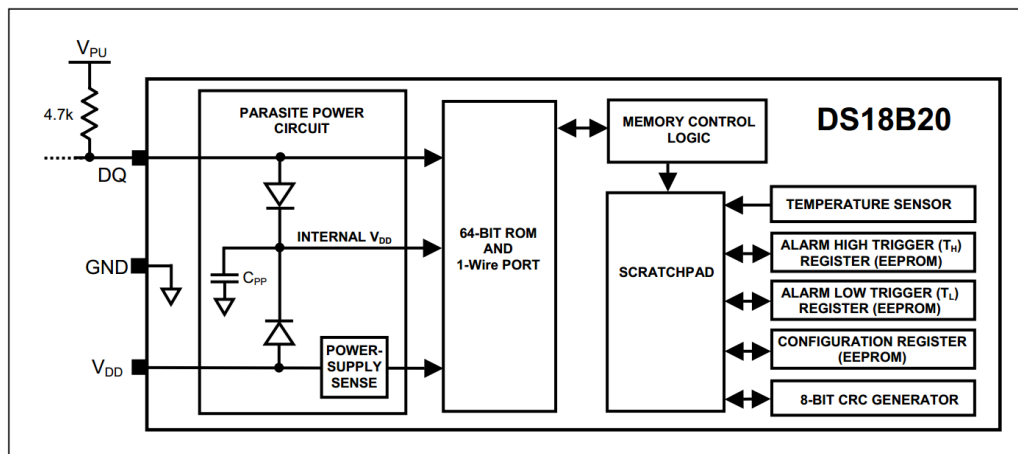


Figure 17. DS18B20 block diagram [20]

The table 3 above shows the basic specification of the temperature sensor DS18B20. The figure 6 above show the block diagram of the sensor. The pin V_{DD} needs to be grounded in parasite power mode for operation. The pin DQ refers to Data Input/Output function. It also provides the power while using in parasite power mode. The pin GND refers to the ground [20].

3.3.3 Signal Processor

The function of the signal processor is processing the data converted by the Photovoltaic Converter and making the data acceptable to PC ground station. It is the key component linking between the PC ground station to UAV sensor.

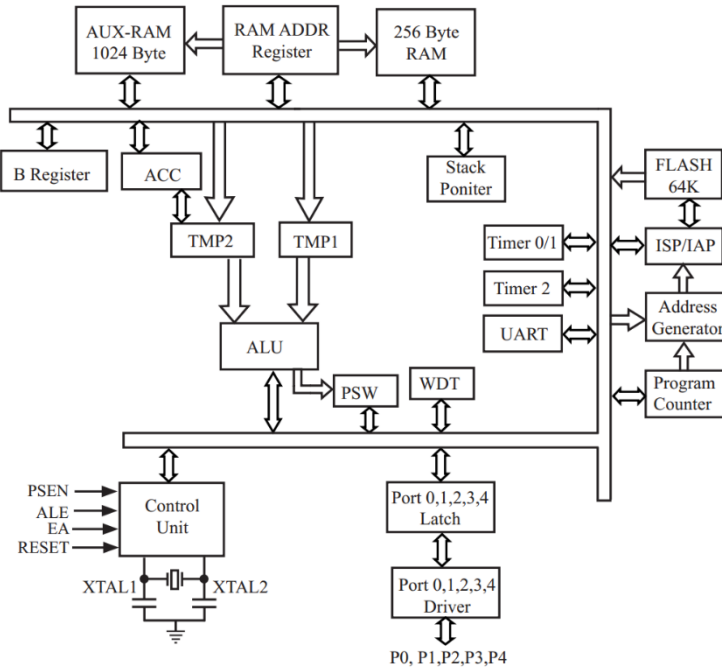


Figure 18. Block diagram of STC89C52

For the temperature communications system, the signal processor should be programmable with industrial-standard and it is able to handle the communication between PC and downlink system. There are many 8-bit and 16-bit microcontroller we can select, such as 80C51, AT89S, Arduino, M6805 and MSP430 [21]. The most popular microchip utilized in Australia is Arduino micro controller, which is widely popularized for building digital devices and interactive objectives. However, the final choice is STC89C52RC microcontroller, not only because it is cheaper and ready to use with inventory on hand, but it is also one of the most famous and mature processors worldwide programmed by C language. It is an 8-bit single chip processor, which has 64K bytes flash memory embedded for programs sharing with in system programming codes. Users can upgrade the program as well as data to In system programming (ISP) and In application programming (IAP). The In system

programming (ISP) allows users to download codes without removing the processor from the end-product. The In application programming (IAP) means the non-volatile data can be written in flash memory when the program is running [22]. 1280 bytes on-chip RAM is provided for wide field application. The following table show the specifications of the processor [23].

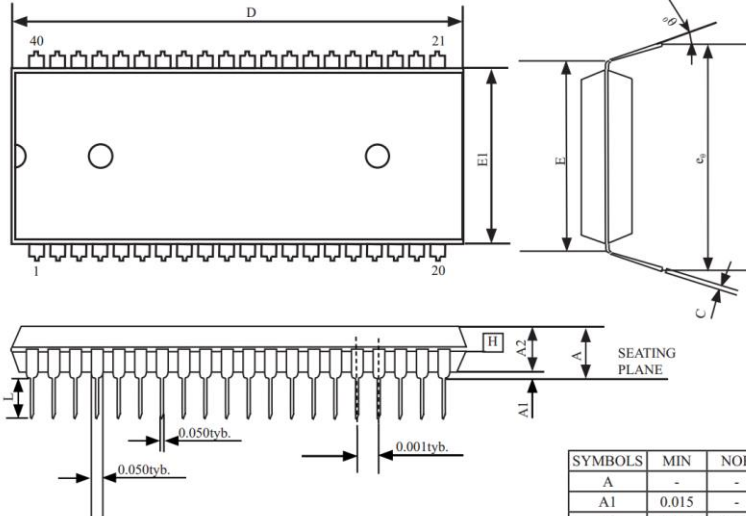
STC89C52RC																																													
Operation voltage range	5.5V ~3.3V																																												
Memory capability	On-chip 4/8/13/16/20/32/64K FLASH																																												
RAM	On-chip 1280 byte / 512 byte																																												
I/O ports	Maximum 39 programmable																																												
Pin assignment	 <table border="1" data-bbox="1214 1336 1483 1560"> <thead> <tr> <th>SYMBOLS</th> <th>MIN</th> <th>NOR</th> <th>MAX</th> </tr> </thead> <tbody> <tr> <td>A</td> <td>-</td> <td>-</td> <td>0.190</td> </tr> <tr> <td>A1</td> <td>0.015</td> <td>-</td> <td>-</td> </tr> <tr> <td>A2</td> <td>0.015</td> <td>0.155</td> <td>0.160</td> </tr> <tr> <td>C</td> <td>0.008</td> <td>-</td> <td>0.015</td> </tr> <tr> <td>D</td> <td>2.025</td> <td>2.060</td> <td>2.070</td> </tr> <tr> <td>E</td> <td></td> <td>0.600</td> <td></td> </tr> <tr> <td>E1</td> <td>0.540</td> <td>0.545</td> <td>0.550</td> </tr> <tr> <td>L</td> <td>0.120</td> <td>0.130</td> <td>0.140</td> </tr> <tr> <td>c₀</td> <td>0.630</td> <td>0.650</td> <td>0.670</td> </tr> <tr> <td>0</td> <td>0</td> <td>7</td> <td>15</td> </tr> </tbody> </table> <p>NOTE: 1.JEDEC OUTLINE :MS-011 AC</p>	SYMBOLS	MIN	NOR	MAX	A	-	-	0.190	A1	0.015	-	-	A2	0.015	0.155	0.160	C	0.008	-	0.015	D	2.025	2.060	2.070	E		0.600		E1	0.540	0.545	0.550	L	0.120	0.130	0.140	c ₀	0.630	0.650	0.670	0	0	7	15
SYMBOLS	MIN	NOR	MAX																																										
A	-	-	0.190																																										
A1	0.015	-	-																																										
A2	0.015	0.155	0.160																																										
C	0.008	-	0.015																																										
D	2.025	2.060	2.070																																										
E		0.600																																											
E1	0.540	0.545	0.550																																										
L	0.120	0.130	0.140																																										
c ₀	0.630	0.650	0.670																																										
0	0	7	15																																										

Table 6. Specifications of 89C52 [23]

3.3.4 USB to TTL converter

The USB refers to Universal Serial Bus. As a standard, it defines the connection and communication between computers and digital devices. It normally has 4 pins, such as voltage supply pin, ground pin, data transmission pin and date receiving pin. Also, it has four transmitting types including interrupt, bulk, ISO and control [24].

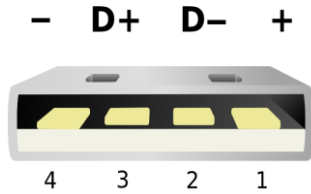


Figure 19. Standard A plug USB

The TTL refers to Transistor-Transistor Logic, which is a type of digital circuit built by resistors and BJTs transistors. It performs both the amplified function and the logic function. Simply speaking, for the processor we selected in this project, the 5V output from the processor pin refers to the logic digital signal “1”, the 0V output from the processor pin refers to the logic digital signal “0”. Since the standard clock oscillator is around 11.0592Mhz to 12Mhz, and the system baud rate is 1/12 of frequency of the oscillator, the baud rate can be approximately calculated as 9600. [25]

The signals transmitted from the sensor will be coded as logic digital signals by the processor and converted to 9600 baud rates which can be acceptable by the PC ground station. In order to make the processor communicate with PC ground station, the USB to TTL converter, also called USB TTL Serial cable should be implemented as the bridge between them. It is a range of USB to serial converter cable which can offer connectivity between serial UART interfaces and USB. Normally, they are operating at 5V or 3.3V with specified signals from various connector interfaces [26].

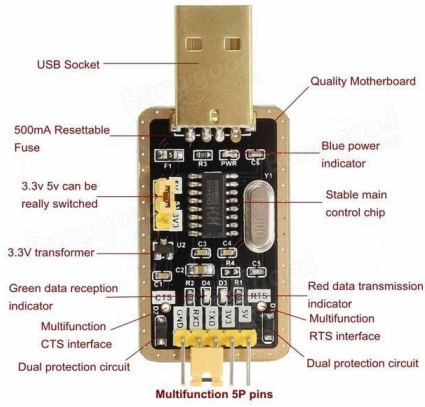


Figure 20. CH340G

There are many types of USB to TTL converters, such as RS232 adaptor, PL2303 converter, CP2102 module serial converter and CH340G converter. In this project, a Universal Asynchronous Receiver / Transmitter (UART), which contains a transmitter (serial to parallel converter) and a receiver (parallel to serial converter), should be utilized to fulfil the requirements of transmitting signals. The CH340G USB to TTL interface converter is selected after compared to other types of converters. The series of CH340 USB bus adaptors can provide serial and parallel interfaces over the USB bus, but the CH340G can only support serial interface only. The reason that it can be selected is because it is cheaper than others and convenient to buy, whilst it is still suited to this project. The specifications of the CH340G is shown in the table below. [25]

Symbol	Name	Minimum	Typical	Maximum	Unit
V _{CC}	Supply rail voltage	4.5	5	5.5	V
I _{CC}	Operating current		12	30	mA
I _{SLP}	Sleeping current		150	200	uA

F _{CLK}	Clock frequency	11.098	12	12.02	MHz
T _{PR}	Power on Reset time		20	50	ms

Table 7. Basic specifications of CH340G [25]

There are five pins available on the CH340G, which are VCC, V3, TxD, RxD, and GND. VCC refers to 5V and V3 refers to 3V power supply from the USB while the V3 pin is not available in the product I brought. The TxD refers to UART data transmit output. The RxD refers to the UART data receive input.

The CH340G requires a 12MHz clock signal during operating. The clock signal is generally provided by load capacitors and a crystal resonator. The clock signal of the CH340H can match the clock signal of the selected processor and the power of the processor can also be supplied by the power from PC ground station through the CH340G.

3.3.5 Circuit & Program design of signal processing

After selected main components of the system, the circuit design was in progress. A testing temperature communication downlink circuit on the breadboard has been built for initially researching the possibility of the design system.

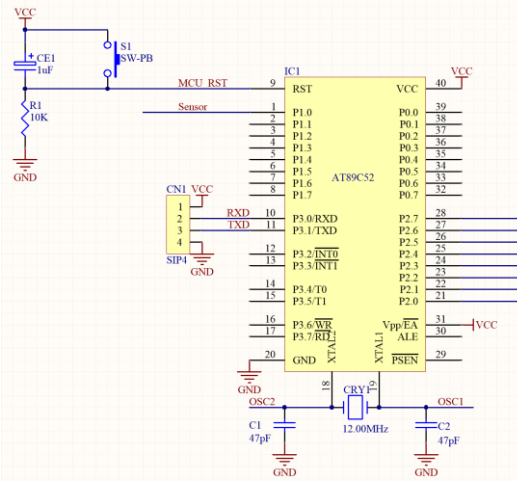


Figure 21. Circuit of the processor [23]

This is the minimized operating system of the processor which connects the temperature sensor and receive 12-bit digital signal from it. The pin 9 connects to the main reset switch paralleling with a 1uF capacitor to VCC. The processor can be reset when the VOH period of RST is greater than two clock cycles. Namely, if the oscillator is 12MHz, the clock cycle is 1us. The VOH period can be calculated as $R*C=10k*1uF=10ms$, which is greater enough to reset the processor. The full page demonstrated the circuit is in the appendix at the end of the report. [27]

The pin 10 and pin 11 are connected to the CH340G for receiving and transmitting data to PC ground station respectively.

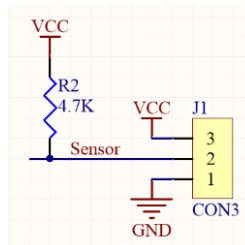


Figure 22. Circuit of the sensor

The temperature is connected according to the datasheet as the circuit shown below. The function of the R2 resistor is limit the current for protecting sensor as well as the processor. [20]

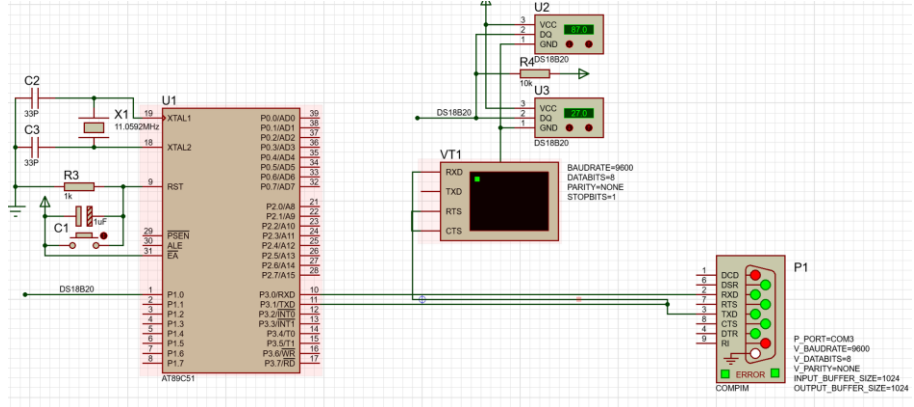


Figure 23. Simulation of the circuit

Before implement the real circuit, simulating the circuit is needed to prove the feasibility and decide the values of elements. The simulated result from Proteus 8 Professional shows the designed circuit can be worked appropriately. However, there was no CH340G component in the electro component library, so an alternative USB to TTL RS232 converter which has the similar functions (RXD and TXD) to CH340G is shown in the figure above.

Also, coding program for processing the sensor signals on the processor is essential and indispensable. The main coding language suited to the processor is C language, which is famous and mature to apply on embedded systems. The development tool is Keil, which is an embedded development tool for a variety of microcontrollers [28].

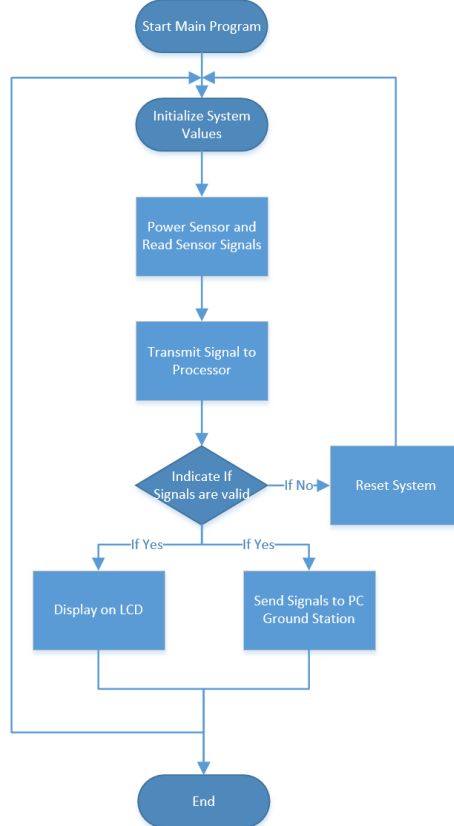


Figure 24. The System Flowchart

The figure above shows the system flow of the signal processing system. The first step of main program is initializing the system values, such as setting pins, and indicate sub-functions. The second step is powering the sensor as well as reading sensor signals function. The third step is transmitting signals to the processor then judge whether the signals are valid or not. If the signals are invalid, the system will be reset and back to the step one. If the signals are valid, two sub-functions, display on LCD and send signals to PC ground station will be activated. After that, the cycle will be broken and back to the first step.

The following codes below shows the sub-function of how the processor reads the order of transforming temperature signals. [29] [30] [31]

```

void Read_Temperature1(void)
//read the temperature from sensor1 and transform signals function;
{
    uchar a,b;

```

```

ds1820rst1(); //reset sensor 2;

ds1820wr1(0xcc); // skip reading serial number;

ds1820wr1(0x44); //start transforming;

ds1820rst1(); //reset sensor 2;

ds1820wr1(0xcc); // skip reading serial number;

ds1820wr1(0xbe); //receive signals;

a=ds1820rd1();

b=ds1820rd1();

CurrentT1=b;

CurrentT1<<=8;

CurrentT1=CurrentT1 | a;

if(CurrentT1<0xffff) tflag1=0;

else{CurrentT1=~CurrentT1+1;tflag1=1;}

CurrentT1=(unsigned int)(CurrentT1*10/16); //transfer hexadecimal to decimalism data;

```

The following codes below shows the sub-function of how the processor sends the temperature signals to PC ground station. [29] [30] [31]

```

void SendTempToPC(unsigned char ch)// the function of sending signals to PC ;

{
    unsigned char i=0;//set initial data i;

    unsigned achs=0,tflag;// set initial system values;

    unsigned int temp=0;//initialise the temperature sensor value;

    switch(ch) //indicate different situations;

    {
        case 1: achs = 'A';tflag=tflag1,temp=CurrentT1;break;// set the situation A;

        case 2: achs = 'B';tflag=tflag2,temp=CurrentT2;break;// set the situation B;

        default: break; //break out the circuit;

    }

    if(ch<5)//indicate whether ch is less than 5;

```

```

{

    SBUF = achs;//give the system value to SBUF;

    while(TI == 0);TI = 0;//do delay (100ms);

    SBUF = '=';//give the value = to SBUF;

    while(TI == 0);TI = 0; //do delay(100ms);

    if(tflag==1) SBUF = '-';// indicate the status of flag and give the system value - to

    SBUF;

    else SBUF = '+';//give the value + to SBUF;

    while(TI == 0);TI = 0;//do delay(100ms);

    SBUF = temp/1000+0x30;      //calculate the Hundreds-digit;

    while(TI == 0);TI = 0;//do delay(100ms);

    SBUF =temp%1000/100+0x30; //calculate the Tens-digit;

    while(TI == 0);TI = 0;//do delay(100ms);

    SBUF =temp%100/10+0x30;   //calculate the Units-digit;

    while(TI == 0);TI = 0;//do delay(100ms);

    SBUF ='.'; //give the value . to SBUF;

    while(TI == 0);TI = 0;//do delay(100ms);

    SBUF =temp%10+0x30;       //calculate the Decimals-digit;

    while(TI == 0);TI = 0;//do delay(100ms);

    SBUF = '\r';//refresh to next line;

    while(TI == 0);TI = 0;//do delay(100ms);

}

else//indicate if ch is larger than 5;

{

    for(i=0;i<8;i++) //do cycle for refreshing screen;

    {

        SBUF = '*';//give the value * to SBUF;

        while(TI == 0);TI = 0;//do delay(100ms);

    }
}

```

```

SBUF = '\r';//refresh to next line
while(TI == 0);TI = 0; //do delay(100ms);
}
ES=1;
EA=1;
delayms(100); //do delay(100ms);
}

```

The following codes below shows the sub-function of how to reset the sensor [29] [30] [31]

```

bit ds1820rst2(void)//reset the sensor 2;
{
    bit x=0;
    DQ2 = 1;      //reset pin DQ2;
    delay_18B20(4); //delay 4ms;
    DQ2 = 0;      //DQ2 off;
    delay_18B20(92); //delay over 480us;
    DQ2 = 1;      //reset pin DQ2;
    delay_18B20(13);
    x=DQ2;        //if DQ2=0, set X=0, initialization succeeded;
    delay_18B20(18);
    return x;
}

```

The completed and integrated code with detailed comments is demonstrated in the appendix.

After stimulated the circuit and tested the code reliability, the constructed circuit is built on a breadboard.

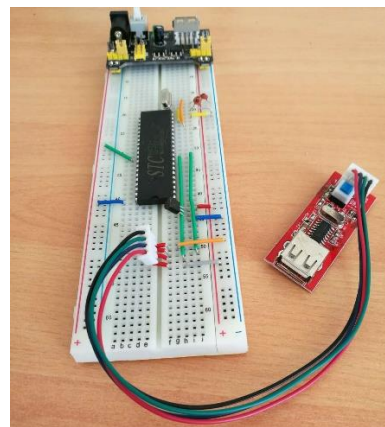


Figure 25. The constructed circuit on breadboard

In order to let PC ground station receive the signal from the CH340G converter, a serial port communication decoder software is needed. This software should have the abilities to searching ports automatically, define baud rate and decode hexadecimal and ASCII data received from the code. There are many choices who have similar functions to each other, such as PortExpert, ComONE, AccessPort, UartAssist, SScom and Comm tunnel [32].

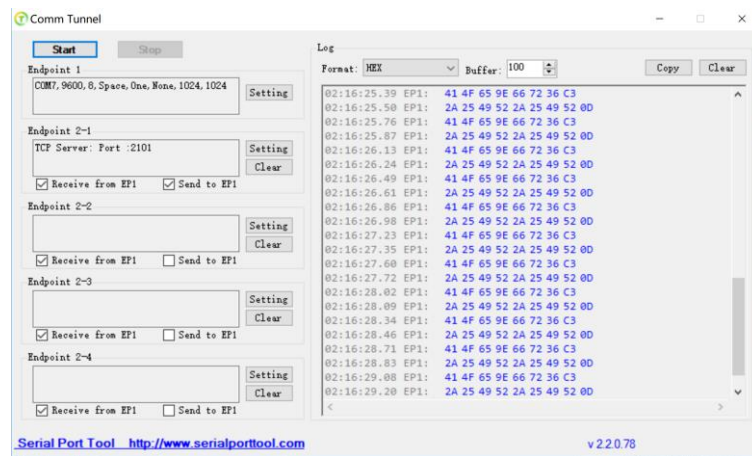


Figure 26. The original hexadecimal data received

The figure above shows the original hexadecimal results received by the PC via the Comm Tunnel Serial Port Debug software. The results are feasible but difficult to read. Since it can only be read with the assistant reference datasheet of DS18B20, there is a need to convert it to the decimal and readable data [33].

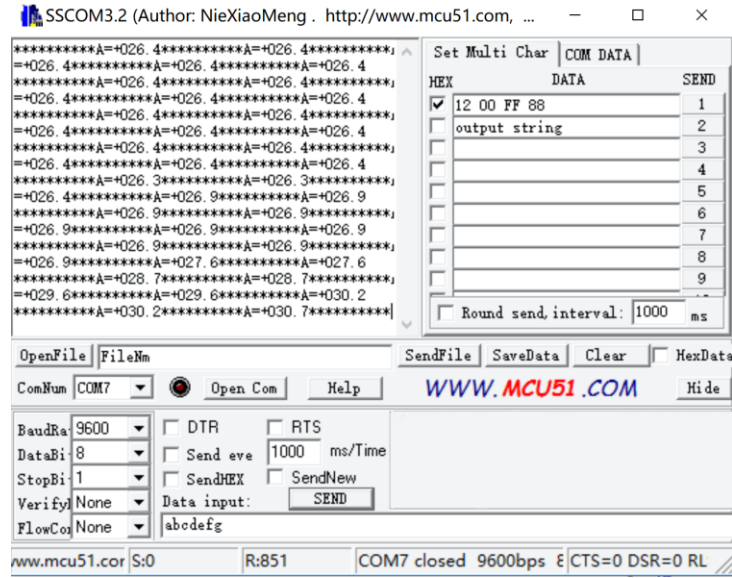


Figure 27. The decoded data received

The figure above shows the decoded decimal data received by the PC via SScom Serial Port Debug software with the 9600 baud rates. And now the data has been converted to decimal data and become more readable. As the figure demonstrated, the data has been changed with the variational temperatures.

The signal processing design was completed on the middle of August 2017.

3.3.6 Further design

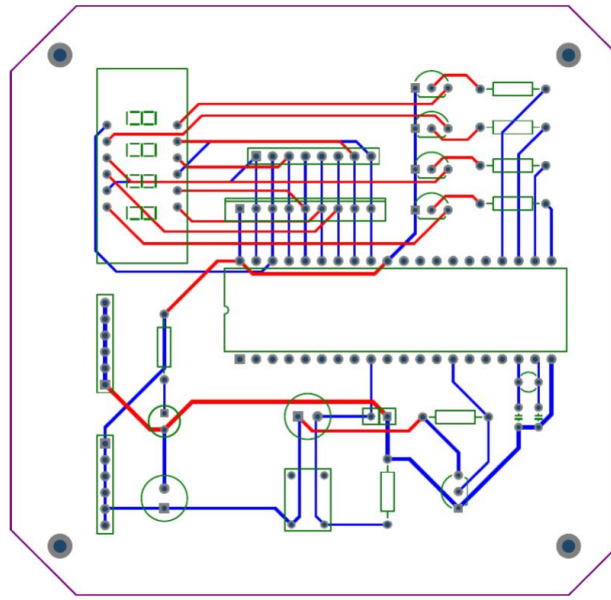


Figure 28. Initial connection scheme of the signal processing system

After completed the signal processing design, the external supervisor Shijie Song advised to do further improvement of the processing system as well as start the optical communication part. The enhanced soldering board was completed based on the previous works.

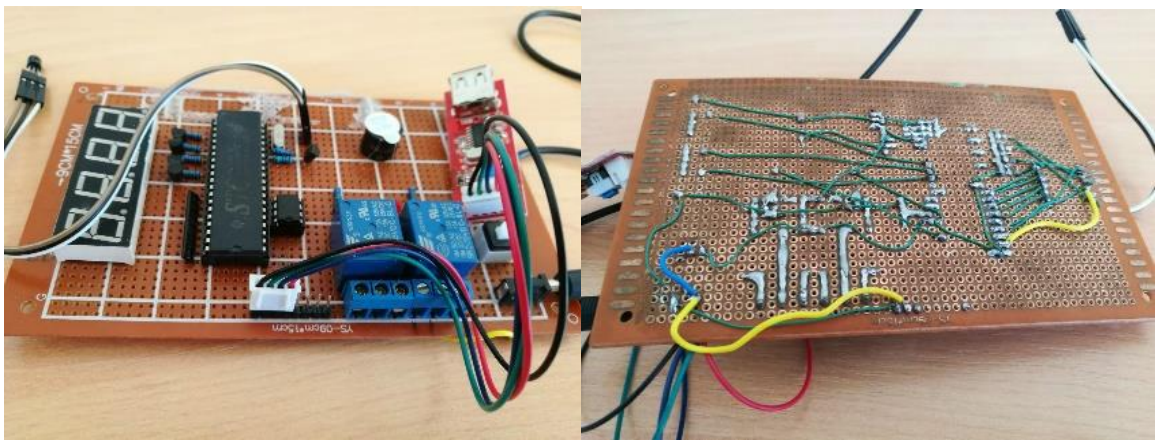


Figure 29. Soldering board temperature signal processing system

The figure above shows the completed welding board temperature signal processing system, it has the similar function to the previous temperature signal processing

system while the difference is that it has the capability to control external relay circuits as well as display the temperature signals both on PC ground station and digital display.

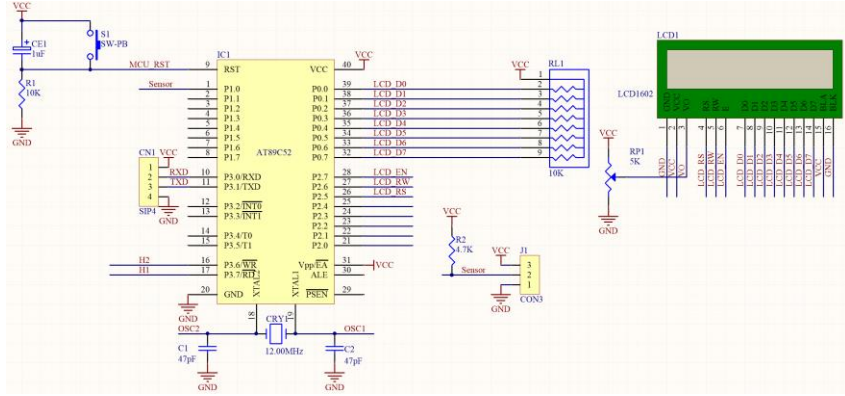


Figure 30. Circuit of the processor with LCD display [34]

The figure above shows the circuit of the processor with LCD display, the pin32 to pin39 are utilized for transmitting data displaying on the screen. Pin26, pin27, and pin 28 are assigned as three control lines referred to as RS, RW, and EN, which are “register select”, “read/write”, and “enable” controls.

The RS can control the data to be approached as a command or an instruction, such as position cursor and clear screen while the voltage value on RS is low (0). When RS is high (0), the screen will display the text data sent from the processor [35].

The RW can control the data bus of the processor. When it is high (1), the processor will read data from LCD. When it is low (0), the data from the processor will be written on the LCD screen. Thus, the voltage value on RW is always low [35].

The EN can control the status of the LCD screen. When it is low (0), the processor is able to send data to the screen and the other control lines will be set and send or receive data to the bus. After the other lines are finished, the voltage value will be

high (1) to wait the minimum time required by the screen then end the cycle through bringing it to low (0) [35].

The welding board temperature signal processing system was completed quickly, and with the assistance from Jianwei Zhai, who is a researcher of South China University of Technology at Guangdong, the PCB of the temperature signal processing system was in progress and finally delivered on 12th Sep 2017.

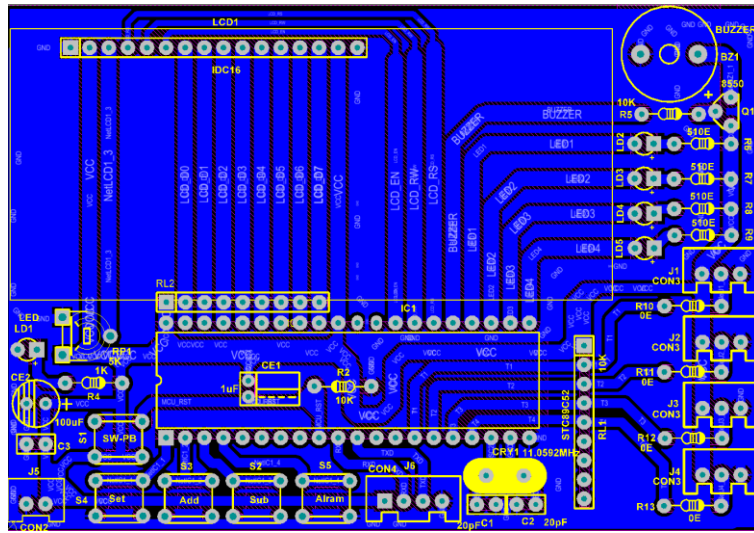


Figure 31. PCB design on Altium Designer

The design of PCB is quite simple since it has only seven normal layers, which are top layer, bottom layer, two mechanical layers, top-over layer keep-out layer and multi-mode layer [36].

The top layer indicates how the components are connecting to others. Namely, it indicates the red lines on the top surface of the PCB [37].

The bottom layer refers to the base level of the PCB, which is shown as the blue colour level. Its function is isolating electronic components on the board [37].

There are two mechanical layers on the design of the PCB. The mechanical layer 1 refers to the soldering points of the back side of the PCB. These soldering points should be exposed to copper surfaces which connected with the lines on the top layer. The mechanical later 2 refers to the toughing points on the front side of the PCB, which would be assembled points of electrical components [37].

The top over layer means the requirement of layouts and spaces of all electronic components on the surface of the PCB. This layer ensures all components would not be overlapped by others on the PCB [37].

The keep-out layer indicates the size of the PCB and the multi-mode layer refers to the number of points that would be connected to the other components outside of the PCB [37].

In order to add the LCD screen function, the following sub-code is added into the main code [37].

```
void Display_Temperature(uint vt,uchar tg,uchar x,uchar y)
// the function of displaying temp;
{
    uchar flagdat;
    disdata[0]=vt/1000+0x30;//calculate and set the Hundreds-digit as disdata0;
    disdata[1]=vt%1000/100+0x30;//calculate and set the Tens-digit as disdata1;
    disdata[2]=vt%100/10+0x30;//calculate and set the Unis-digit as disdata2;
    disdata[3]=vt%10+0x30;//calculate and set the Decimals-digit as disdata2;
    if(tg==0)  flagdat=43;//if the temperature is positive, no plus sign;
    else  flagdat=0x2d;//if the temperature is negative, display minus sign;
    writeChar(x,y,flagdat);//display sign on x,y position;
    writeChar(x+1,y,disdata[0]);//display Hundreds-digit on x+1,y position;
    writeChar(x+2,y,disdata[1]);//display Tens-digiton x+2,y position;
```

```

        writeChar(x+3,y,disdata[2]);//display Unis-digit on x+3,y position;
        writeChar(x+4,y,0X2E); //display a point on x+4,y position;
        writeChar(x+5,y,disdata[3]); //display Decimals-digit on x+5,y position;
    }

```

Since then, the main code functionalities, such as reading and transferring signals from the sensor, sending signals to PC ground station, and displaying data on the LCD screen, have been achieved. The integrated code, which includes basic setting of system pins, is shown in the appendix while it may have a few differences due to the dissimilar format and the further optimization.

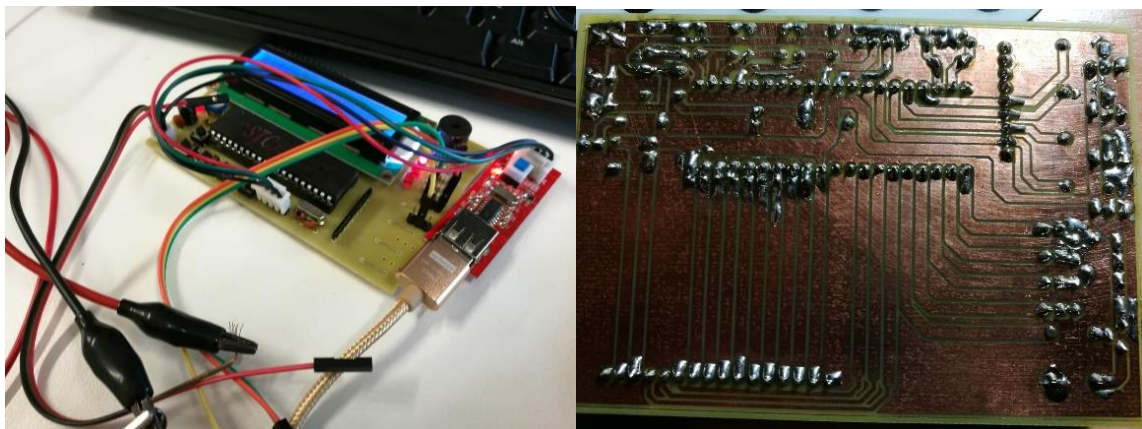


Figure 32. PCB of the temperature signal processing system

The PCB is in well working condition and has the same operating principles to previous works. The design of PCB is shown in the figure above as well as in the appendix.

However, the finally delivered PCB is not exactly the same to the designed board. The J3 and J4 connectors for additional sensors are not soldered on the board.

3.3.7 Light source

The light source takes the responsibility for There are two available led sources we can utilize on the Dimoto kit provided by the external supervisor. The one is red led,

which has 660 nm peak wavelength, 20 nm spectral bandwidth, 0.1 us rising time and 0.1 falling time. The other one is green led, which has 530 nm peak wavelength, 50 nm spectral bandwidth, 3.5 ns rising time and 16 ns falling time.

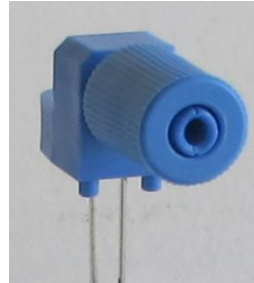


Figure 33. IF E93

The IF-E93 housed in a connector less style package is utilized to generate the green led output, and the spectrum is generated by gallium nitride die peaking at 522nm wavelength. It is ideal to map the PMMA plastic optical fibre at the lowest attenuation window. An internal LED micro-lens is contained in the device package. The efficiency of optical coupling can be ensured by the PBT plastic housing with the standard 1000 μm core plastic fiber cables. The features of IF-E93E, such as high output and fast transition times make it suited to low cost digital data links. Its attenuation is less than 1db/m while coupling to PMMA plastic optical fibre. The data rates are up to 5Mbps and the operating distance is up to 150 meters when using 1mm standard core plastic fibre. Thus, this light source is suited to the project. The characteristics of IF-E93 are shown in the table below. [38]

Parameter	Symbol	Min	Typ	Max	Unit
Peak Wavelength	λ_{PEAK}	-	522	-	nm
Spectral Bandwidth (FWHM)	$\Delta\lambda$	-	40	-	nm

Output Power Coupled into Plastic Fiber	P _O	600 -2.2	790 -1.0	950 -0.2	μW dBm
Switching Times	tr, tf	-	145, 80	-	ns
Capacitance	C ₀	-	65	-	pF
Forward Voltage	V _f	-	3.1	-	V

Table 8. Characteristics of IF E93 (TA = 25°C)

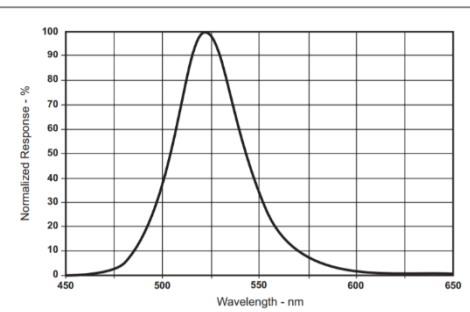


Figure 34. Forward current vs. forward voltage [38]

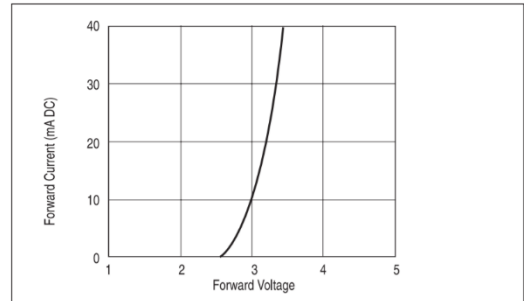


Figure 35. Typical spectral output vs. wavelength [38]

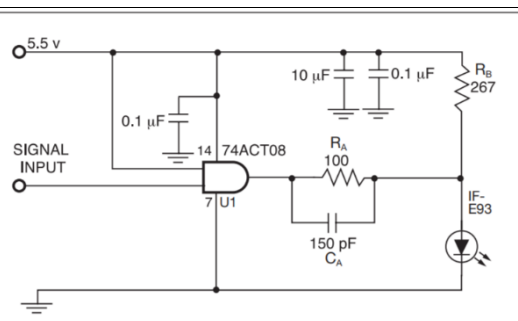


Figure 36. Test/Application circuit (IF = 33mA) [38]

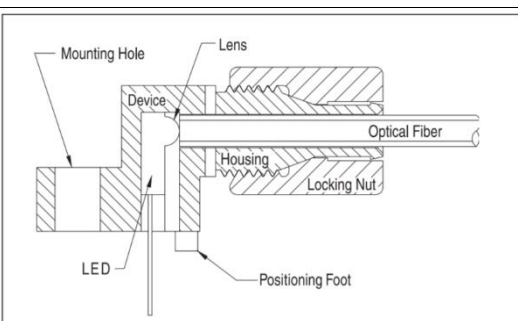


Figure 37. Cross-section of fiber optic device [38]

Table 9. Features of IF-E93 led [38]

3.3.8 Photovoltaic converters

The photovoltaic converters are available on the Dimoto kit which is provided by the external supervisor. The photovoltaic converters include optical to electrical converter (O/E) and electrical to optical (E/O) converter. The functions of these photovoltaic converters are converting digital signals from the sensor to optical signals for transmitting via optical fibre, and then receive the optical signals as well as convert them to electrical signals for digital signal processing on the processor [39]. The E/O converter is considered as the LED source which has been demonstrated in the section above. The O/E converter, IF D96F is selected and shown in the figure below.



Figure 38. IF D96F

The IF-D96F housed in a connector less style package is utilized as a medium-speed photo detector. An IC with a photodiode, voltage comparator, linear amplifier and Schmitt trigger logic circuit are contained in the detector. An Schottky transistor output of an inverted open-collector is featured by the IF-D96F. 5TTL loads over output voltage between 4.5V to 15V can be drove by this device. It is especially suited to digital data links at 5Mbps rates. The noise immunity and the TTL/COMS can be improved by a Schmitt trigger with existing digital circuit. The stable operation and wide dynamic range can be ensured by an enhanced internal electrical architecture. Thus, the IF-D96F has the capability to provide a variety of cost-effective digital applications, especially in this project [40].

Parameter	Symbol	Min	Typ	Max	Unit
Peak Sensitivity	λ_{PEAK}	—	700	—	nm
Spectral Sensitivity	$\Delta\lambda$	500	—	780	nm
Recommended Operating Voltage	VCC	4.5	-	15.0	V
High Level Supply Current	I _{CCH}	—	3.5	6	mA
Low Level Supply Current	I _{CCL}	—	12	14.5	mA
Light Level to Trigger (RL=1 kΩ λ =650 nm)	Er (+)	—	7 -21.6	-	μ W dBm
Hysteresis Ratio	Er(+)/Er(-)	—	1.1	—	—
High Level Output Current	I _{OH}	—	5	100	μ A
Low Level Output Voltage	V _{OL}	—	0.1	0.55	V

Table 10. Characteristics of IF D96F (TA=25°C) VCC = 4.75 to 5.25 V [40]

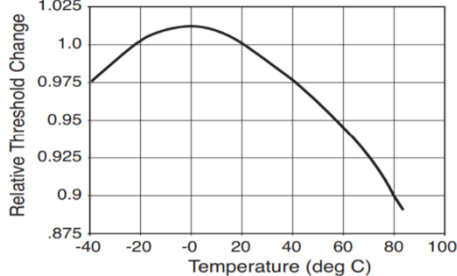


Figure 39. Normalized threshold irradiance vs. amb. temp [40]

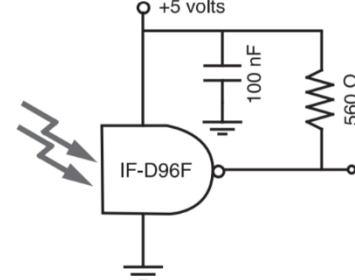


Figure 40. Typical operating circuit [40]

3.3.9 Final version control

After combined all components into an integrated system, the final version of the temperature communication optical downlink system is shown in the figure below.

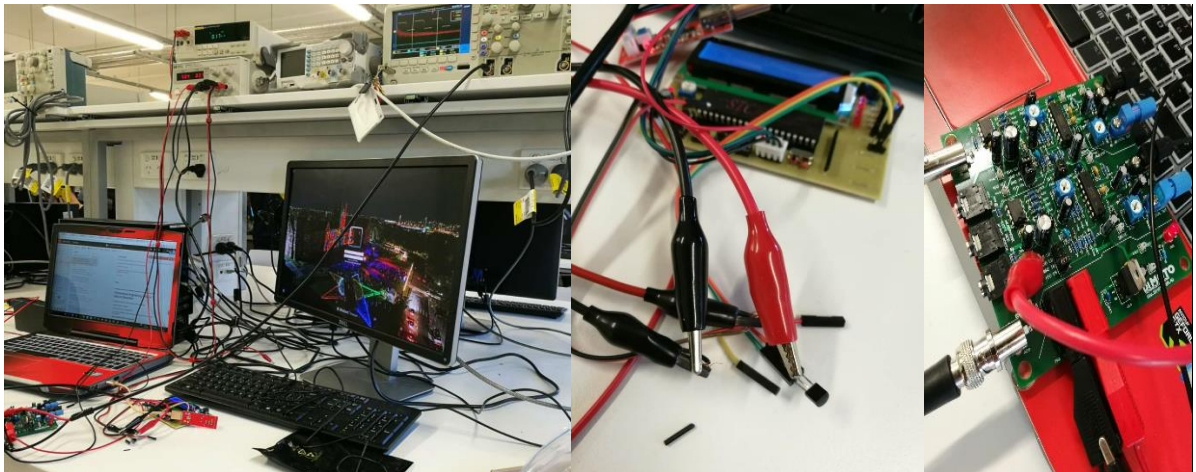


Figure 41. Integrated temperature communication optical downlink system

The Integrated temperature communication optical downlink system is in a well working condition in the experimental environment. The PCB of the processor and the sensor are powered by the lab power supply. The output pin DQ of the sensor is connected to the BNC input pin of the Dimoto board while the signals from the sensor is now seemed as analog signals. The Dimoto board will convert the electrical signals to optical signals by the IF E93 and send them through a plastic fibre then receive them by the IF D96F. However, the output of the O/E converter IF D96F is

over than 5V, which is not acceptable to the processor. Thus, the output of IF D96F will be tested by the oscilloscope and demonstrated how the digital output varied with the variation of the temperature.

3.3.10 Conclusion



Figure 42. The system scheme of temperature downlink communication system

The whole system can be described as the figure above.

The temperature communication optical downlink system was completed on 16 Oct 2017. Although the total amount of data transferring in this system is less than the video communication optical downlink system, the degree of difficulty is much harder than the previous one since the underlying signal processing is an additional work which raises the difficulty level to the project. Finally, threes working temperature signal processing system have successfully completed and one demonstrable integrated temperature communication optical downlink system is set, analysed and tested in the experimental environment.

The utilized system components except lab facilities include: DS18B20, STC89C52, CH340G, breadboard, soldering board, PCB, IF E93, IF D96F, dimoto board, and several electronic components such as wires, resistances, oscillators, capacitors, etc.

4. Analysis & Test

4.1 Original Outputs from The Temperature Sensor

The lab results were obtained on 16th Oct 2017 and 18th Oct 2017, which were the first opening day and the second opening day of the laboratory. The original outputs from the sensor are shown below.



Figure 43. The output of the sensor
(18.2 °C)

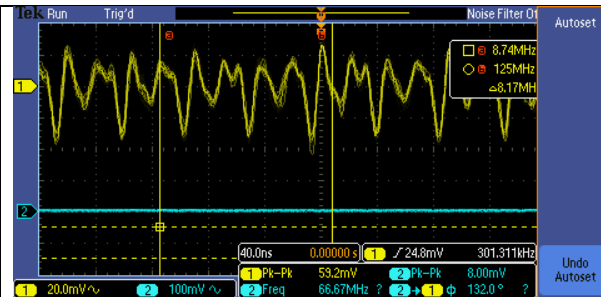


Figure 44. The output of the sensor
(18.5 °C)

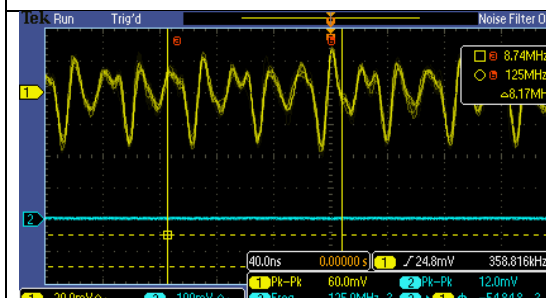


Figure 45. The output of the sensor
(18.7 °C)

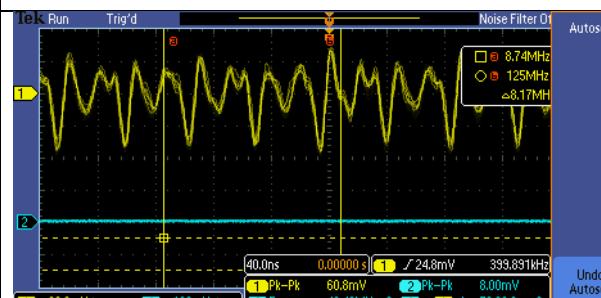


Figure 46. The output of the sensor
(19.0 °C)



Figure 47. The output of the sensor
(19.3 °C)

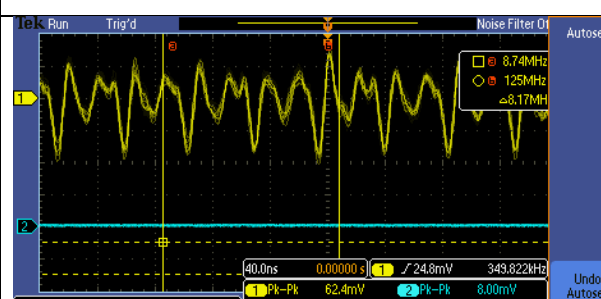


Figure 48. The output of the sensor
(19.5 °C)

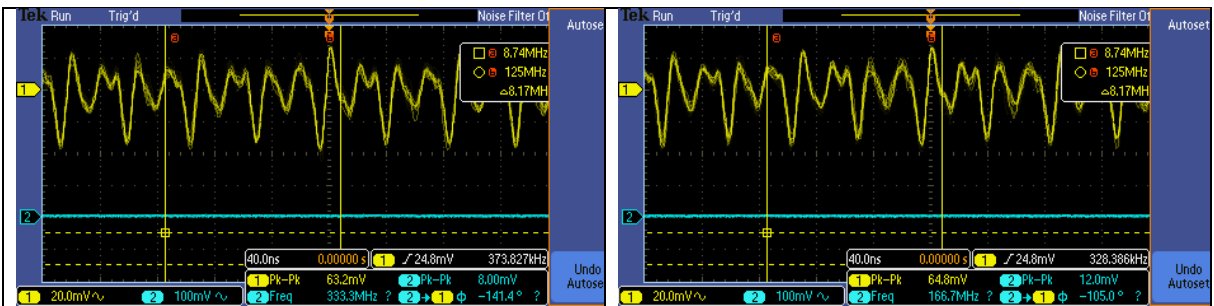


Figure 50. The output of the sensor
(20.3 °C)

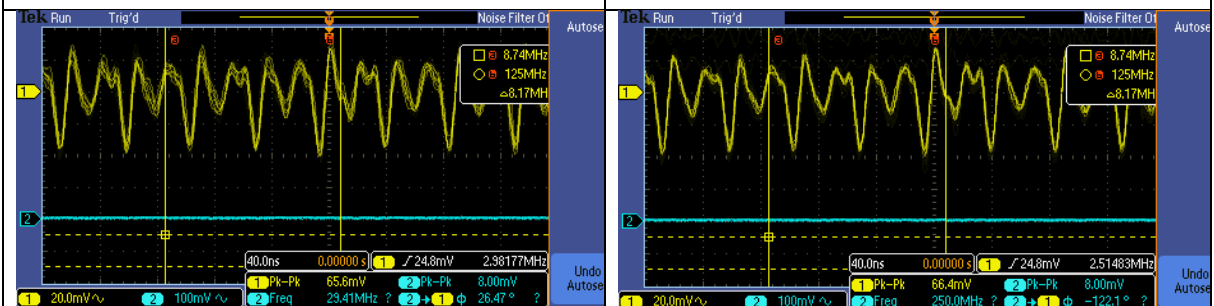


Figure 52. The output of the sensor
(20.7 °C)

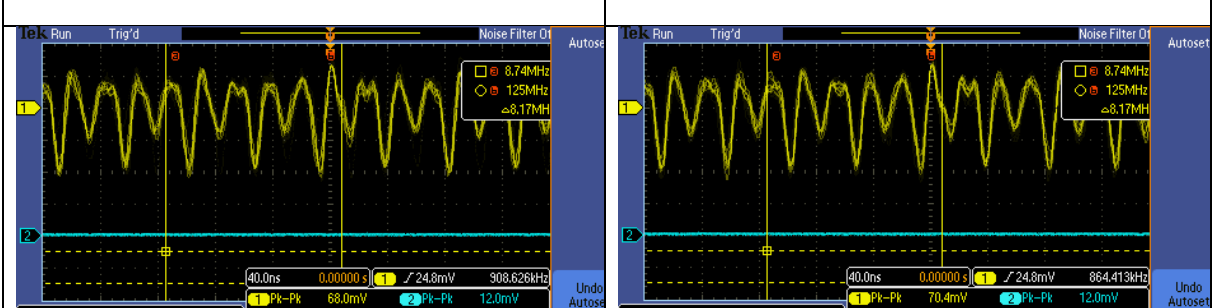


Figure 54. The output of the sensor
(22.0 °C)

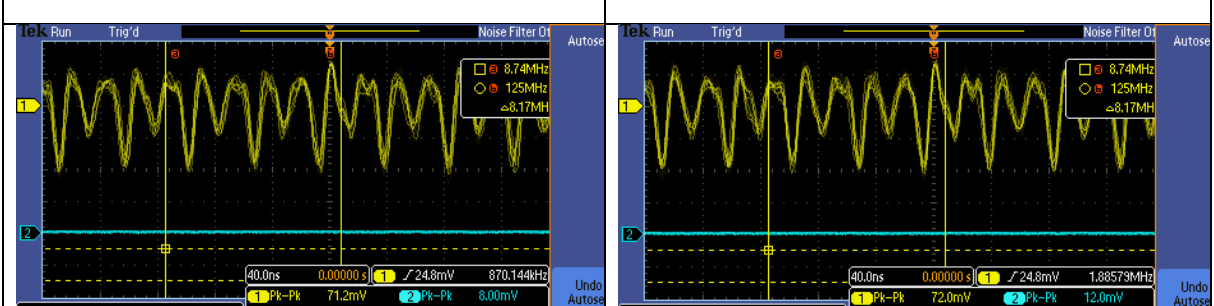


Figure 56. The output of the sensor
(22.5 °C)

The original outputs of the sensor indicate that the output voltage is increasing constantly with the increase of the environment temperature. The relation between them is shown in the figure below.

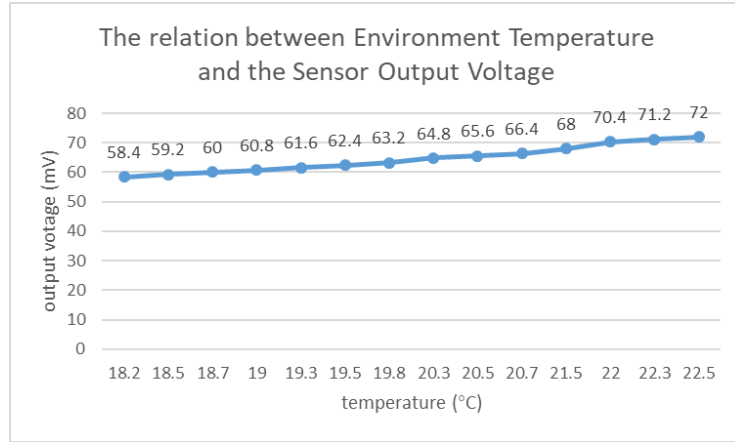


Figure 57. Environment Temperature V.S. the Sensor Output Voltage

The relation between the DQ output voltage and the environment temperature can be indicated as the following equation.

$$T \text{ (}^{\circ}\text{C)} = \frac{V_{pk-pk}}{2} * 0.625 \text{ (mV)}$$

4.2 Converted output from the IF D96F

Since the temperature signals are converted to optical signals and received by the IF D96F, the amplified outputs of the IF D96F can demonstrate whether the temperature downlink communications system is working or not.



Figure 58. The output of the IF D96F (18.5 °C)

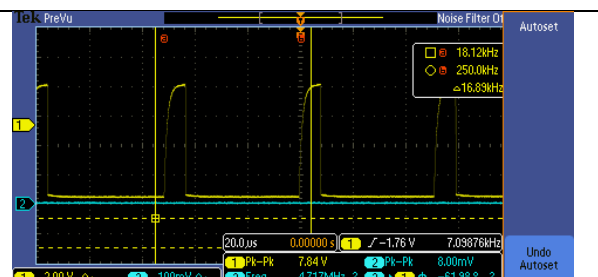


Figure 59. The output of the IF D96F (20.5 °C)

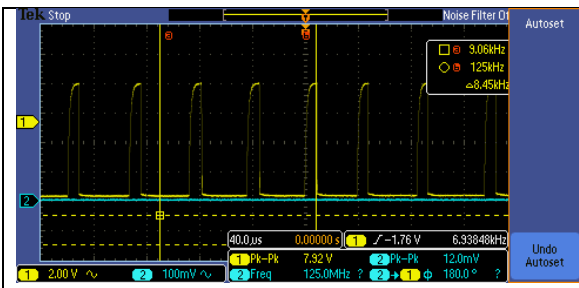


Figure 60. The output of the IF D96F
(22.5 °C)

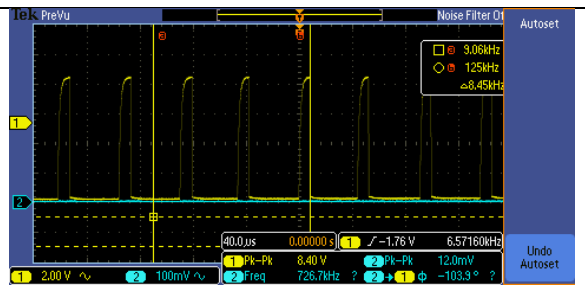


Figure 61. The output of the IF D96F
(24.5 °C)

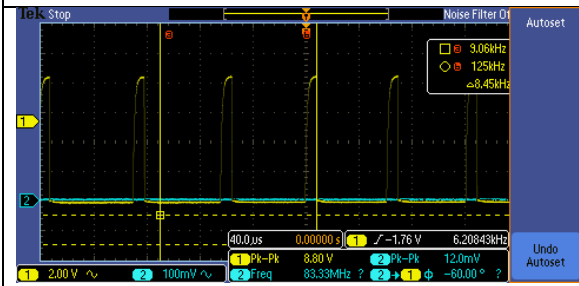


Figure 62. The output of the IF D96F
(26.5 °C)

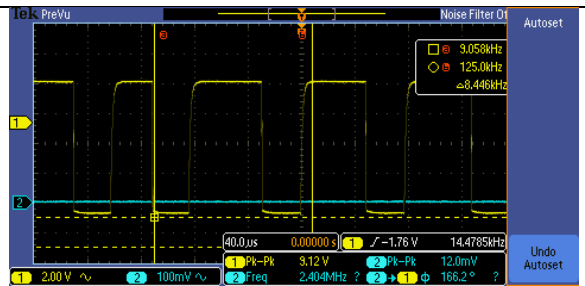


Figure 63. The output of the IF D96F
(28.5 °C)

As we can see from the lab results, the outputs of IF D96F are amplified and modified to digital signals which can be decoded to temperature signals again. The modified outputs of the converter indicate that the output voltage is increasing constantly with the increase of the environment temperature. The average gain is calculated as 115.693 V/V.

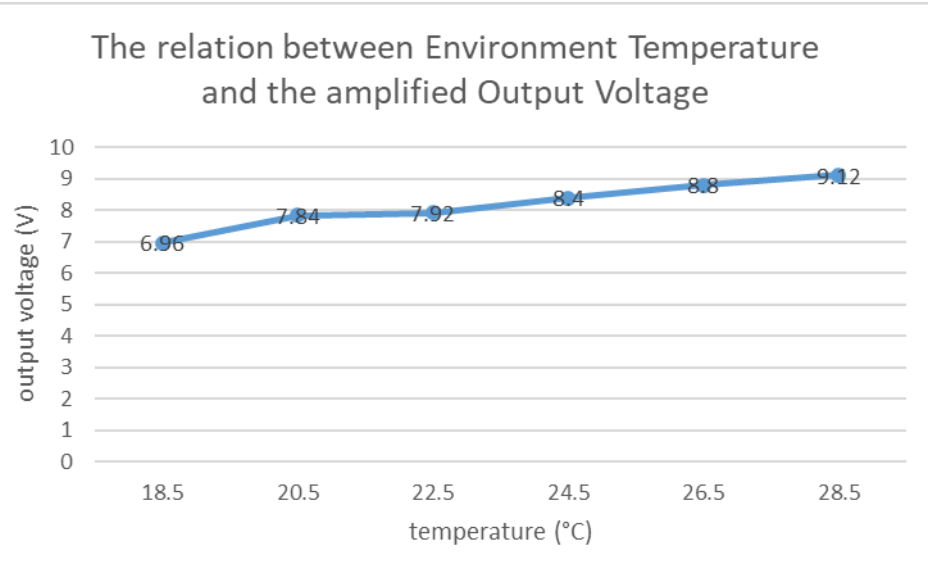


Figure 64. Environment Temperature V.S. the amplified Output Voltage

5. Conclusion

5.1 Completed works

Since the mainstream UAV system has a series of defects, the main idea of this project is optimizing the UAV via photovoltaic technologies. For examples, the mainstream drones are usually powered by a 3S battery with a limited working period (normally from 5 mins to 20 mins) and the control system of wireless drones is easily affected by Electro-Magnetic Interference (EMI). Thus, the goals of the project are researching and analysing the possibility of how to utilize the photovoltaic technologies to overcome the weaknesses of the mainstream UAV system.

The works contained in this project include several recent advanced technologies related to electrical engineering and optoelectronics, such as the laser power over fibre (POF), optical-to-electrical (O/E) and electrical-to-optical (E/O) conversion, the DC voltage conversion, the underlying signal processing, C programming and the PCB design.

However, there are many difficulties during the process of implementing our ideas in practice. Although it is feasible to supply drones through laser power over fibre after carefully researched the market and theoretically analysed its possibility, the potential risk of operating such a high-power laser source and the exorbitant purchase costs become a huge stumbling block. Also, the PCB design was prolonged due to the lack of supports and the strangeness of local market.

Fortunately, the barriers did not block the project since our supervisors provided an alternative way and additional supports to complete tasks.

5.2 Future work

There are a few issues that have not been solved, such as safely implementing the high-power laser on drones, sending laser power and transmitting data with one multi-mode fibre to minimize the load, and the experiment as well as analysis of the underlying signal processing of the video downlink communication system.

For improving the transmission data rate, there are several advanced technologies are recommended to apply on the UAV system. For example, Free-space optical (FSO) communication is an optical communication technology using light propagating in free space to transmit data wirelessly with very high data rates (up to Gbps) [41]. It can improve the data transmitting speed and the limited carrying load of the UAV as well as minimize the influence of EMI. The Acoustic charge transport(ACT) processor, which has the ability to enable users to sample a time signal without quantized the sample amplitude, can be helpful to resist radio interference [42]. Moreover, the laser radar can also be utilized on UAV for measuring terrain at night and communication with other UAV [43].

6. Appendix

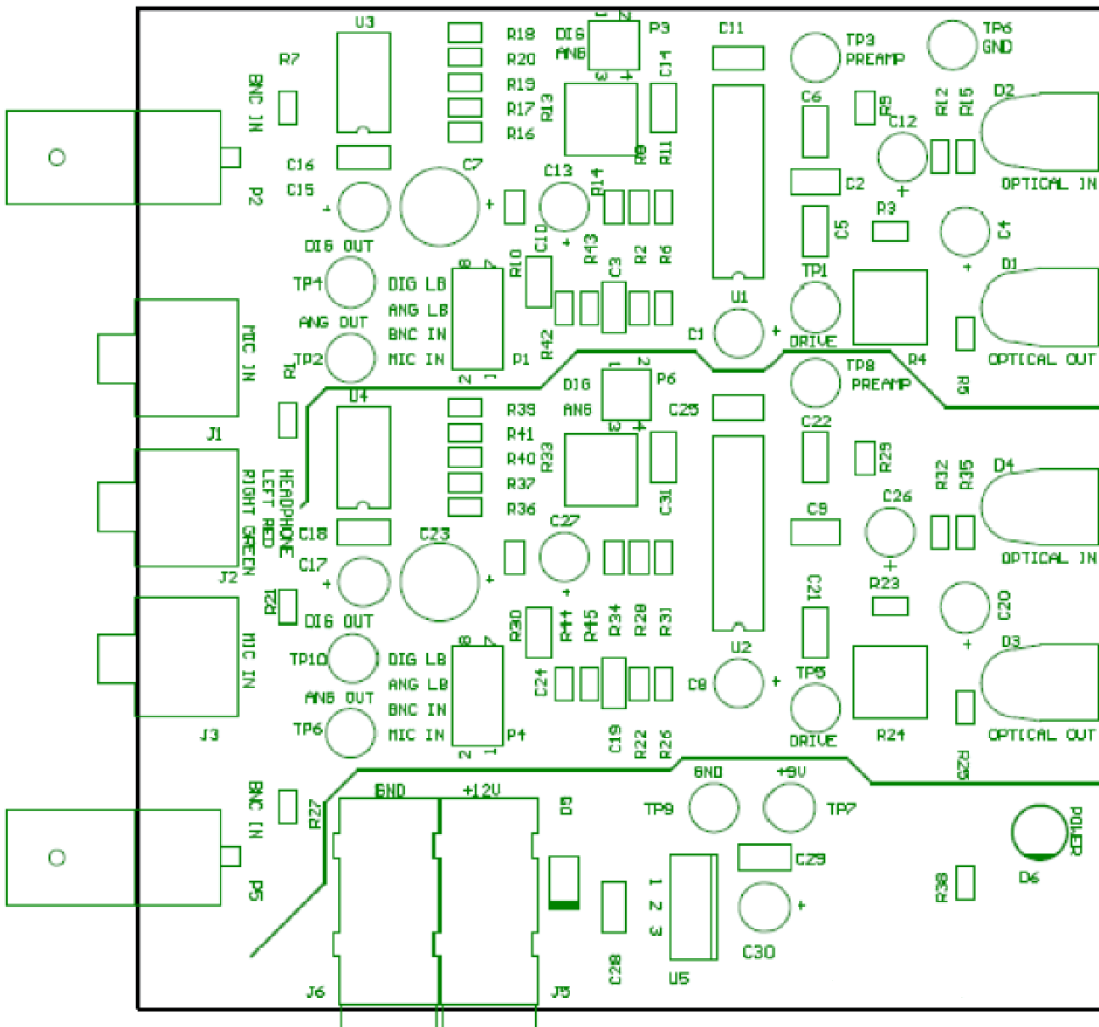


Figure 65. PCB layout of DIMOTO board

The whole code below is original program with detailed notes written by C language applied on the final version of the temperature signal processing of the downlink system.

```
#include <intrinsics.h>
#include <reg52.h>
#define uint unsigned int
#define uchar unsigned char
```

```
sbit DQ2=P3^5;//set the pin 35 of processor to connect with the sensor;  
sbit DQ1=P3^4;//set the pin 34 of processor to connect with the sensor;  
sbit LED4 = P2^0;//set the pin 20 of processor to connect with the EN of LCD;  
sbit LED3 = P2^1;//set the pin 21 of processor to connect with the EN of LCD;  
sbit LED2 = P2^2;//set the pin 22 of processor to connect with the EN of LCD;  
sbit LED1 = P2^3;//set the pin 23 of processor to connect with the EN of LCD;  
sbit RS=P2^5;//set the pin 25 of processor to connect with the RS of LCD;  
sbit RW=P2^6;//set the pin 26 of processor to connect with the RW of LCD;  
sbit EN=P2^7;//set the pin 27 of processor to connect with the EN of LCD;
```

```
uchar data disdata[5];  
uint CurrentT1=0,CurrentT2=0;// initial temperature values;  
bit tflag1,tflag2,tflag3,tflag4;//the sign of temperature values;  
bit ch1=1,ch2=1;  
unsigned char chs=0;  
unsigned char Alarm1=0,Alarm2=0;//initial alarm value  
unsigned char ts=0;
```

```
#define LCD_BUS P0  
unsigned char fAlarm=0;  
unsigned char AlarmTempLow=20, AlarmTempTop=35,Set=0,NG=0;  
//set the upper and lower alarm temperature values, while it is useless in this project;
```

```
void SendTempToPC(unsigned char ch);  
void delayms(uint ms) //set delay sub-function;  
{  
    uchar i;  
    while(ms--)  
    {  
        for(i=0;i<100;i++) //set a delay cycle
```

```

    }

}

void command(uint com) //set command sub-funtion
{
    RS=0;           // register select, clear screen
    LCD_BUS=com;   // set bus with commands
    delayms(5);    //set delay for 5ms then enable
    EN=1;
    delayms(5);    //set delay for 5ms then disable
    EN=0;
}

void write_dat(uchar dat) // write data function;
{
    RS=1;           // register select, clear screen;
    LCD_BUS=dat;   //set bus with data;
    delayms(5);    //set delay for 5ms then enable;
    EN=1;
    delayms(5);    //set delay for 5ms then disable;
    EN=0;
}

void writestring(uchar x,uchar y,uchar *s) //write characters on the screen function;
{
    if (y == 0) command(0x80 + x); //if y position is 0, write in the first line;
    else     command(0xC0 + x); //else write in the second line;

    while (*s)           // judging cycle of whether it is the end of characters;
    {

```

```

    write_dat( *s);

    s++;
}

}

void writeChar(uchar x,uchar y,uchar s) // write the characters;
{
    if (y == 0) command(0x80 + x); //if y position is 0, write in the first line;
    else      command(0xC0 + x); //else write in the second line;
    {
        write_dat( s); // display the current character
    }
}

void LCD_Initial() //initialise LCD
{
    EN=0;                      //LCD off
    RW=0;                      //RW off
    command(0x38);             // initial command
    command(0x0c);
    command(0x06);
    command(0x01);
    command(0x80);
}

void Usart_Initial(void) //initialise the values of serial interface;
{
    TMOD = 0x20; // set the mode of Timer;
    SCON = 0x50;// serial control register
    PCON = 0x00;
}

```

```

    TL1 = 0xfd;// determine the baud rate of UART for Timer
    TH1 = 0xfd; // determine the baud rate of UART for Timer
    EA = 1;
    ES = 1;
    TR1 = 1;
    delayms(100);

}

void SendTempToPC(unsigned char ch)// the function of sending signals to PC ;
{
    unsigned char i=0;//set initial data i;
    unsigned achs=0,tflag;// set initial system values;
    unsigned int temp=0;//initialise the temperature sensor value;
    switch(ch) //indicate different situations;
    {
        case 1: achs = 'A';tflag=tflag1,temp=CurrentT1;break;// set the situation A;
        case 2: achs = 'B';tflag=tflag2,temp=CurrentT2;break;// set the situation B;
        default: break; //break out the circuit;
    }
    if(ch<5)//indicate whether ch is less than 5;
    {
        SBUF = achs;//give the system value to SBUF;
        while(TI == 0);TI = 0;//do delay (100ms);
        SBUF = '=';//give the value = to SBUF;
        while(TI == 0);TI = 0; //do delay(100ms);
        if(tflag==1) SBUF = '-';
        // indicate the status of flag and give the system value - to SBUF;
        else SBUF = '+';//give the value + to SBUF;
        while(TI == 0);TI = 0;//do delay(100ms);
    }
}

```

```

SBUF = temp/1000+0x30;      //calculate the Hundreds-digit;
while(TI == 0);TI = 0;//do delay(100ms);
SBUF =temp%1000/100+0x30; //calculate the Tens-digit;
while(TI == 0);TI = 0;//do delay(100ms);
SBUF =temp%100/10+0x30;    //calculate the Units-digit;
while(TI == 0);TI = 0;//do delay(100ms);
SBUF ='.'; //give the value . to SBUF;
while(TI == 0);TI = 0;//do delay(100ms);
SBUF =temp%10+0x30;        //calculate the Decimals-digit;
while(TI == 0);TI = 0;//do delay(100ms);
SBUF = '\r';//refresh to next line;
while(TI == 0);TI = 0;//do delay(100ms);
}

else//indicate if ch is larger than 5;
{
    for(i=0;i<8;i++) //do cycle for refreshing screen;
    {
        SBUF = '*';//give the value * to SBUF;
        while(TI == 0);TI = 0;//do delay(100ms);
    }
    SBUF = '\r';//refresh to next line
    while(TI == 0);TI = 0; //do delay(100ms);
}
ES=1;
EA=1;
delayms(100); //do delay(100ms);
}

void delay_18B20(unsigned char i)

```

```

{
    while(i--);
    delay_18B20(4); //delay 4ms;
}

bit ds1820rst1(void)//reset the sensor;
{
    bit x=0;
    DQ1 = 1;      //reset pin DQ;
    delay_18B20(4);
    DQ1 = 0;      //DQ off;
    delay_18B20(92); //delay over 80ms;
    DQ1 = 1;      ///reset pin DQ agian;
    delay_18B20(13);
    x=DQ1;        //if DQ=0, set X=0, initialization sucessed;
    delay_18B20(18);
    return x;
}

```

```

uchar ds1820rd1(void)//read data function for sensor 1;
{
    unsigned char dat = 0;// set the value of dat;
    unsigned char i=0;// set the values of i;
    for (i=8;i>0;i--) // input data to a byte (8bit)
    {
        DQ1 = 0; //pulse sensor signals;
        dat>>=1; //move the data to lower order;
        DQ1 = 1; //pulse sensor signals;
        if(DQ1) //if there is a sensor output;
        dat|=0x80; //save the data to the highest order;
}

```

```

        delay_18B20(9);

    }

    return(dat);
}

void ds1820wr1(uchar wdata) // write data function for sensor 1;
{
    unsigned char i=0; // set the values of i;
    for (i=8; i>0; i--) // input data to a byte (8bit)
    {
        DQ1 = 0;//pulse sensor signals;
        DQ1 = wdata&0x01;//write data to the highest order;
        delay_18B20(9);
        DQ1 = 1;
        wdata>>=1; //move the data to lower order;
    }
}

bit ds1820rst2(void)//reset the sensor 2;
{
    bit x=0;
    DQ2 = 1;      //reset pin DQ2;
    delay_18B20(4); //delay 4ms;
    DQ2 = 0;      //DQ2 off;
    delay_18B20(92); //delay over 480us;
    DQ2 = 1;      //reset pin DQ2;
    delay_18B20(13);
    x=DQ2;      //if DQ2=0, set X=0, initialization sucessed;
    delay_18B20(18);
    return x;
}

```

```

}

uchar ds1820rd2(void)//read signals function for sensor 2;
{
    unsigned char dat = 0;// set the value of dat;
    unsigned char i=0;// set the values of i;
    for (i=8;i>0;i--) // input data to a byte (8bit)
    {
        DQ2 = 0; //pulse sensor signals;
        dat>>=1; //move the data to lower order;
        DQ2 = 1; //pulse sensor signals;
        if(DQ2) //if there is an output from sensor2;
        dat|=0x80; //save the data to the highest order;
        delay_18B20(9);
    }
    return(dat);
}

```

```

void ds1820wr2(uchar wdata)//write signals function for senor 2;
{
    unsigned char i=0; // set the values of i;
    for (i=8; i>0; i--) // input data to a byte (8bit)
    {
        DQ2 = 0;//pulse sensor signals;
        DQ2 = wdata&0x01;//write data to the highest order;
        delay_18B20(9);
        DQ2 = 1;
        wdata>>=1; //move the data to lower order;
    }
}

```

```

void Read_Temperature1(void)
//read the temperature from sensor1 and transform signals function;
{
    uchar a,b;

    ds1820rst1(); //reset sensor 2;

    ds1820wr1(0xcc);// skip reading serial number;

    ds1820wr1(0x44);//start transforming;

    ds1820rst1(); //reset sensor 2;

    ds1820wr1(0xcc); // skip reading serial number;

    ds1820wr1(0xbe);//receive signals;

    a=ds1820rd1();

    b=ds1820rd1();

    CurrentT1=b;

    CurrentT1<<=8;

    CurrentT1=CurrentT1 | a;

    if(CurrentT1<0xffff) //indicate whether it is valid

        tflag1=0;

    else{

        CurrentT1=~CurrentT1+1;tflag1=1; }

        CurrentT1=(unsigned int)(CurrentT1*10/16);//(0.625));

        //transfer hexadecimal to decimalism data;

    }
}

```

```

void Read_Temperature2(void)//read the temperature sensor and transform signals;
{
    uchar a,b;

    ds1820rst2(); //reset sensor 2;

    ds1820wr2(0xcc);// skip reading serial number;

    ds1820wr2(0x44);//start transforming;

```

```

ds1820rst2(); // reset sensor 2;
ds1820wr2(0xcc); // skip reading serial number;
ds1820wr2(0xbe); // receive signals;
a=ds1820rd2();
b=ds1820rd2();
CurrentT2=b;
CurrentT2<<=8;
CurrentT2=CurrentT2|a;
if(CurrentT2<0xffff) tflag2=0;
else {CurrentT2=~CurrentT2+1;tflag2=1;}
CurrentT2=(unsigned int)(CurrentT2*10/16); // transfer hexadecimal to
decimalism data;
}


```

```

void Display_Temperature(uint vt, uchar tg, uchar x, uchar y)
// the displaying function;
{
    uchar flagdat;
    disdata[0]=vt/1000+0x30; // calculate and set the Hundreds-digit as disdata0;
    disdata[1]=vt%1000/100+0x30; // calculate and set the Tens-digit as disdata1;
    disdata[2]=vt%100/10+0x30; // calculate and set the Unis-digit as disdata2;
    disdata[3]=vt%10+0x30; // calculate and set the Decimals-digit as disdata2;
    if(tg==0) flagdat=43; // if the temperature is positive, no plus sign;
    else flagdat=0x2d; // if the temperature is negative, display minus sign;
    writeChar(x,y,flagdat); // display sign on x,y position;
    writeChar(x+1,y,disdata[0]); // display Hundreds-digit on x+1,y position;
    writeChar(x+2,y,disdata[1]); // display Tens-digit on x+2,y position;
    writeChar(x+3,y,disdata[2]); // display Unis-digit on x+3,y position;
    writeChar(x+4,y,0X2E); // display a point on x+4,y position;

```

```

        writeChar(x+5,y,disdata[3]);//display Decimals-digit on x+5,y position;
    }

void OneSensor(void) //only one sensor connected;
{
    if(ch1==0)    // if sensor1 connected;
    {
        Read_Temperature1();//go to go to read signals function for sensor 1;
        Display_Temperature(CurrentT1,tflag1,7,0); //go to display function;
        SendTempToPC(1); //go to send to PC function;
    }
    if(ch2==0)    // if sensor2 connected;
    {
        Read_Temperature2();//go to read signals function for sensor 1;
        Display_Temperature(CurrentT2,tflag2,7,0);//go to display function;
        SendTempToPC(2);//go to send to PC function;
    }
}

void TwoSensor(void) //two sensors connected;
{
    if(ch1==0) // if sensor1 connected;
    {
        Read_Temperature1();//go to read signals function for sensor 2;
        Display_Temperature(CurrentT1,tflag1,1,0); //go to display function;
        SendTempToPC(1);//go to send to PC function;
    }
    else(ch2==0) // else if sensor2 connected;
    {
        Read_Temperature2();    //go to read signals function for sensor 2;
        Display_Temperature(CurrentT2,tflag2,10,0); //go to display function;
    }
}

```

```

        SendTempToPC(2);//go to send to PC function;
    }

}

void DisplaySensor(void)//display the number of sensor function;
{
    switch(chs)
    {
        case 1:
        {
            writestring(0,0," CurT=      "); //display temperature characters
            }break;

        case 2:
        {
            if(ch1==0)
            {
                writestring(0,0,"A"); //sensor A displayed
                if(ch2==0) writestring(9,0,"B");//sensor B displayed
            }
            else if(ch2==0)
            {
                writestring(0,0,"B"); //only sensor B displayed
            }
            }break;
    }
}

```

```

void CheckSensor(void)// check whether sensors are connected
{

```

```

ch1=0;ch2=0;

chs=0;

ch1=ds1820rst1();

ch2=ds1820rst2();

delayms(200);

if(ch1==0) {chs++;}
if(ch2==0) {chs++;}

writestring(0,1," Get Sensor ");writeChar(6,1,chs+'0');delayms(1000);

// display get sensors

while(chs==0) writestring(0,0," No Sensor ");

writestring(0,0,"");
writestring(0,1,"");

DisplaySensor(); //go to DisplaySensor

}

void main(void) //main function
{
    unsigned char i=0;
    P2=0xff; //set 8pins of p2 of the processor as high;
    LCD_Initial(); //initial LCD;
    Read_Temperature1(); //go to Read_Temperature1 function1;
    Read_Temperature2(); // go to Read_Temperature1 function2;

    writestring(0,0," DS18B20 "); //display DS18B20'
    Usart_Initial();
    delayms(1000); //delay 1S
    writestring(0,0,""); //dispaly space on x=0,y=0
    writestring(0,1,""); //dispaly space on x=0,y=1

```

```
CheckSensor();  
  
NG=0;  
if(Set==0)  
{  
    if(chs==1) //one sensor connected  
    {  
        OneSensor(); //go to onesensor function  
    }  
    if(chs==2) //two sensors connected  
    {  
        TwoSensor(); //go to twosensor function  
    }  
}  
}
```

7. Bibliography

- [1] V. Sittakul et al, "Power-over-fibre for wireless applications," *Microwave and Optical Technology Letters*, vol. 53, (5), pp. 1027-1032, 2011..
- [2] DBMTEAM, "13 Best Drones With The Longest Flight Time," 5 2 2017. [Online]. Available: <http://dronebusinessmarketer.com/best-drones-with-longest-flight-time/>.
- [3] BEACONTEAM, "fios.verizon.com," THE BEACON, 23 4 2015. [Online]. Available: <https://fios.verizon.com/beacon/fiber-optics-vs-coaxial-cables/>.
- [4] M. Shalaby et al, "Evaluation of Electromagnetic Interference in Wireless Broadband Systems," *Wireless Personal Communications*, vol. 96, (2), pp. 2223-2237, 2017..
- [5] simtoo, "http://www.simtoo.com," [Online]. Available: <http://www.simtoo.com/page.php?id=132#page1>. [Accessed 30 04 2017].
- [6] I. V. Yakovlev, "Stretchers and compressors for ultra-high power laser systems," *Quantum Electronics*, vol. 44, (5), pp. 393-414, 2014..
- [7] T. Ōkoshi, *Optical Fibers*. 2012..
- [8] J. Piprek, "Analysis of efficiency limitations in high-power InGaN/GaN laser diodes," *Optical and Quantum Electronics*, vol. 48, (10), pp. 1-8, 2016..
- [9] azastra, "http://www.azastra.com," [Online]. Available: <http://www.azastra.com/6-volt.html>. [Accessed 04 05 2017].
- [10] F. L. Luo, H. Ye and ProQuest (Firm), *Advanced DC/DC Converters*. (Second ed.) 2017..
- [11] digikey, "www.digikey.com.au," [Online]. Available: <https://www.digikey.com.au/product-detail/en/ge-critical-power/APXW012A0X3-SRZ/555-1374-1-ND/5168590>. [Accessed 05 05 2017].

- [12] A. Sivapriya and A. Sivanantharaja, "Uplink and downlink of RF signals using optical frequency multiplication in radio over fiber," in 2013, . DOI: 10.1109/ICICES.2013.6508389..
- [13] Thunderbolt, "<http://www.corning.com>," Thunderbolt, [Online]. Available: <http://www.corning.com/optical-cables-by-corning/worldwide/en.html>. [Accessed 23 5 2017].
- [14] Anonymous "DBPOWER UDI U818A Wifi, FPV Quadcopter with headless mode and HD Camera," M2 Presswire, 2017..
- [15] Alex, "dronetrest," unmannedtech, 05 11 2015. [Online]. Available: <http://www.dronetrest.com/t/fpv-cameras-for-your-drone-what-you-need-to-know-before-you-buy-one/1441>. [Accessed 23 6 2017].
- [16] Helipal, "<http://www.helipal.com>," Helipal, [Online]. Available: http://www.helipal.com/product_info.php?currency=AUD&products_id=14561&gclid=CjwKCAjwmqHPBRBQEiwAOvbR8502RcolUxPvdtUxfjBhAYT5iZGFS-02HO_Saebwnk7o0TAAkpZOlxoC2kEQAvD_BwE. [Accessed 20 07 2017].
- [17] Helipal, "<http://www.helipal.com>," Helipal, [Online]. Available: http://www.helipal.com/product_info.php?currency=AUD&products_id=15425&gclid=CjwKCAjwmqHPBRBQEiwAOvbR82m39quRMJk5InqkMFZ3F2IgaV7x6BQ5nTnSg_5-8-mq7JrlJecMRoCD7MQAvD_BwE. [Accessed 25 7 2017].
- [18] N. Dey, A. Mukherjee and Ebooks Corporation, Embedded Systems and Robotics with Open Source Tools. 2016..
- [19] S. F. Li and L. Yang, "Application of Distributed Measurement and Control System," Applied Mechanics and Materials, vol. 385-386, pp. 504, 2013..
- [20] Y. Wu, "c.biancheng.net," [Online]. Available: <http://c.biancheng.net/cpp/html/1958.html>. [Accessed 20 07 2017].
- [21] J. P. Agrawal and T. V. Nahar, Microcontroller and Embedded Systems. (Second ed.) London, UK: New Academic Science, 2017..

- [22] S. B. Qi, M. Zhang and Z. H. Wang, "Remote Multi-Processor Updating System Based on In-System Programming and CAN-Bus," *Applied Mechanics and Materials*, vol. 364, pp. 419, 2013..
- [23] Y. Wu, "<http://c.biancheng.net/>," [Online]. Available: <http://c.biancheng.net/cpp/html/1856.html>. [Accessed 20 07 2017].
- [24] K. Yokoyama, Y. Tsuchida and T. Gokan, "Optical & non-contact data transmission system with input through USB port of personal computer," *Seimitsu Kogaku Kaishi/Journal of the Japan Society for Precision Engineering*, vol. 74, (8), pp. 825-829, 2008..
- [25] DreamCity, "<http://www.foxdelta.com/>," [Online]. Available: <http://www.foxdelta.com/products/ST2-0816/ch340g.pdf>. [Accessed 20 09 2017].
- [26] J. K. a. D. J. R. Radan Slavík, "Feed-forward true carrier extraction of high baud rate phase shift keyed signals using photonic modulation stripping and low-bandwidth electronics," *Optics Express*, vol. 19, no. 27, 2011.
- [27] i. maxim, "www.maximintegrated.com/," [Online]. Available: <https://www.maximintegrated.com/en/products/analog/sensors-and-sensor-interface/DS18B20.html>. [Accessed 20 09 2017].
- [28] D. Ibrahim, PIC Microcontroller Projects in C: Basic to Advanced. (2nd ed.) 2014..
- [29] 21ic, "www.21ic.com/," [Online]. Available: <http://www.21ic.com/jichuzhishi/datasheet/DS18B20/chengxu/185326.html>. [Accessed 25 08 2017].
- [30] G. YANG, "wenku.baidu.com/," 13 08 2010. [Online]. Available: <https://wenku.baidu.com/view/691f0f85ec3a87c24028c416.html?from=search>. [Accessed 25 08 2017].
- [31] L. L. Zhenyu GU, "Port Design of DS18B20 with C," *SWIC*, vol. 7, pp. 22-24, 2002.
- [32] T. Malinowski, "Tools of the Serials Trade," *Serials Review*, vol. 39, (3), pp. 211-213, 2013..

- [33] D. Ibrahim, Designing Embedded Systems with 32-Bit PIC Microcontrollers and MikroC. 2013..
- [34] resource, “<http://www.8052.com>,” [Online]. Available: <http://www.8052.com>. [Accessed 01 9 2017].
- [35] D. Ibrahim, Using LEDs, LCDs, and GLCDs in Microcontroller Projects. 2012..
- [36] Think58, “<http://www.think58.com>,” think58, [Online]. Available: <http://www.think58.com/elec/24251.html>. [Accessed 20 8 2017].
- [37] R. Murugan et al, "Improving microcontroller (MCU) immunity performance to system-level ESD/EFT testing through PCB system co-design methodology," in 2014, ..
- [38] d. G, “i-fiberoptics.com,” [Online]. Available: <http://i-fiberoptics.com/pdf/ifd93f.pdf>. [Accessed 18 10 2017].
- [39] Anonymous "Canare Showcases AES-3id Electrical-to-Optical and Optical-to-Electrical Converters at AES," Business Wire, 2012..
- [40] Ddimoto, “i-fiberoptics.com,” [Online]. Available: <http://i-fiberoptics.com/pdf/ifd96f.pdf>. [Accessed 10 10 2017].
- [41] C. L. H. W. J. W. J. C. Ruhai Guo, “Protocol Design for Free Space Optical (FSO) Communication,” *Applied Mechanics and Materials*, pp. 1178-1184, 3 2015.
- [42] S. Zheng et al, "Acoustic charge transport induced by the surface acoustic wave in chemical doped graphene," Applied Physics Letters, vol. 109, (18), pp. 183110, 2016..
- [43] K. Chiang et al, "Development of LiDAR-Based UAV System for Environment Reconstruction," IEEE Geoscience and Remote Sensing Letters, vol. 14, (10), pp. 1790-1794, 2017..